TKK Dissertations 141
Espoo 2008

# AUTOTHERMAL REFORMING OF SIMULATED AND COMMERCIAL FUELS ON ZIRCONIA-SUPPORTED MONO- AND BIMETALLIC NOBLE METAL CATALYSTS

Doctoral Dissertation

**Reetta Kaila**

**Helsinki University of Technology**
**Faculty of Chemistry and Materials Sciences**
**Department of Biotechnology and Chemical Technology**

TKK Dissertations 141
Espoo 2008

# AUTOTHERMAL REFORMING OF SIMULATED AND COMMERCIAL FUELS ON ZIRCONIA-SUPPORTED MONO- AND BIMETALLIC NOBLE METAL CATALYSTS

Doctoral Dissertation

**Reetta Kaila**

Dissertation for the degree of Doctor of Science in Technology to be presented with due permission of the Faculty of Chemistry and Materials Sciences for public examination and debate in Auditorium KE2 (Komppa Auditorium) at Helsinki University of Technology (Espoo, Finland) on the 24th of October, 2008, at 12 noon.

**Helsinki University of Technology**
**Faculty of Chemistry and Materials Sciences**
**Department of Biotechnology and Chemical Technology**

**Teknillinen korkeakoulu**
**Kemian ja materiaalitieteiden tiedekunta**
**Biotekniikan ja kemian tekniikan laitos**

Distribution:
Helsinki University of Technology
Faculty of Chemistry and Materials Sciences
Department of Biotechnology and Chemical Technology
P.O. Box 6100
FI - 02015 TKK
FINLAND
URL: http://chemat.tkk.fi/
Tel. +358-9-4511
E-mail: reetta.kaila@nesteoil.com



ISBN 978-951-22-9570-8
ISBN 978-951-22-9571-5 (PDF)
ISSN 1795-2239
ISSN 1795-4584 (PDF)
URL: http://lib.tkk.fi/Diss/2008/isbn9789512295715/

TKK-DISS-2512

Multiprint Oy
Espoo 2008

| ABSTRACT OF DOCTORAL DISSERTATION | HELSINKI UNIVERSITY OF TECHNOLOGY<br>P.O. BOX 1000, FI-02015 TKK<br>http://www.tkk.fi |
|---|---|

Author Reetta Kaila

Name of the dissertation
Autothermal reforming of simulated and commercial fuels on zirconia-supported mono- and bimetallic noble metal catalysts


| Manuscript submitted May 23, 2008 | Manuscript revised September 26, 2008 |
|---|---|
| Date of the defence October 24, 2008 | |
| ☐ Monograph | ☒ Article dissertation (summary + original articles) |

| | |
|---|---|
| Faculty | Faculty of Chemistry and Materials Sciences |
| Department | Department of Biotechnology and Chemical Technology |
| Field of research | Industrial Chemistry |
| Opponent(s) | Prof. Anders Holmen |
| Supervisor | Prof. Outi Krause |
| Instructor | Prof. Outi Krause |



Abstract

New energy sources are needed if energy supply and demand are to remain in balance. At the same time, the level of emissions needs to be reduced to minimise their contribution to the greenhouse effect. Renewable energy sources, and hydrogen ($H_2$), have been attracting much attention, and more efficient technologies for energy recovery have been developed. Among these are fuel cells.

$H_2$ is not a source of energy but an energy carrier, which needs to be produced from a primary fuel (hydrocarbons, alcohols, water). Conventionally $H_2$ is produced by steam reforming (SR) of natural gas. For mobile applications, however, a liquid fuel that is easy to deliver and safe to store is at present more feasible. Since the reaction enthalpy of SR increases markedly with the length of the hydrocarbon chain of the fuel, autothermal reforming (ATR), where endothermic SR is combined with exothermic partial oxidation (POX), is preferable to conventional SR.

ATR of hydrocarbon fuels was investigated for the on-site production of $H_2$-rich fuel gas suitable for solid oxide fuel cell (SOFC) applications. ATR of commercial fuels has to be carried out at high temperatures (700–900 °C) to achieve complete conversion of both the aliphatic and aromatic hydrocarbon fractions. With high temperature, however, thermal reactions of aliphatic hydrocarbons accelerate producing undesired compounds that also promote coke formation. These challenges can be overcome with active, selective and stable catalysts.

$ZrO_2$-supported mono- and bimetallic noble metal (Rh, Pd, Pt) catalysts were examined. Rh proved to be most active for SR, whereas Pt was active for oxidation reactions. The good features of these two metals were combined in the bimetallic catalysts where strong synergism exists between Rh and Pt. Catalytic performance was excellent, there were no side products and coke formation was suppressed. Furthermore, ATR of commercial low-sulfur diesel was successfully carried out on these bimetallic RhPt catalysts, which exhibited high thermal stability even in the presence of heterocyclic sulfur compounds.



Keywords hydrogen production, autothermal reforming, liquid hydrocarbon fuels, noble metal catalysts, zirconia support

| | | | |
|---|---|---|---|
| ISBN (printed) | 978-951-22-9570-8 | ISSN (printed) | 1795-2239 |
| ISBN (pdf) | 978-951-22-9571-5 | ISSN (pdf) | 1795-4584 |
| Language | english | Number of pages | 71 p. + app. 41 p. |

| | |
|---|---|
| Publisher | Helsinki University of Technology, Department of Biotechnology and Chemical Technology |
| Print distribution | Helsinki University of Technology, Department of Biotechnology and Chemical Technology |

The dissertation can be read at http://lib.tkk.fi/Diss/2008/isbn9789512295715/

| VÄITÖSKIRJAN TIIVISTELMÄ | TEKNILLINEN KORKEAKOULU<br>PL 1000, 02015 TKK<br>http://www.tkk.fi |
|---|---|

Tekijä Reetta Kaila

Väitöskirjan nimi
Simuloitujen ja kaupallisten polttoaineiden autoterminen reformointi mono- ja bimetallisilla jalometalli-$ZrO_2$ -katalyyteillä

| Käsikirjoituksen päivämäärä 23.5.2008 | Korjatun käsikirjoituksen päivämäärä 26.9.2008 |
|---|---|

Väitöstilaisuuden ajankohta 24.10.2008

| ☐ Monografia | ☒ Yhdistelmäväitöskirja (yhteenveto + erillisartikkelit) |
|---|---|

| | |
|---|---|
| Tiedekunta | Kemian ja materiaalitieteiden tiedekunta |
| Laitos | Biotekniikan ja kemian tekniikan laitos |
| Tutkimusala | Teknillinen kemia |
| Vastaväittäjä(t) | Prof. Anders Holmen |
| Työn valvoja | Prof. Outi Krause |
| Työn ohjaaja | Prof. Outi Krause |


Tiivistelmä

Kasvihuonekaasujen muodostusta on vähennettävä ilmastonmuutoksen hillitsemiseksi. Yksi merkittävimmistä kasvihuonekaasuista on hiilidioksidi ($CO_2$), jota syntyy eniten energian tuotannosta, liikenteestä ja teollisuudesta. Koska energian kysyntä kasvaa jatkuvasti, on uusia energianlähteitä ja puhtaampia tuotantotapoja kehitettävä. Uusiutuvat energiamuodot ja mm. vety- ja polttokennoteknologiat ovatkin herättäneet kiinnostusta tekemällä puhtaamman energiantuotannon mahdolliseksi. Vety itsessään ei kuitenkaan ole energialähde vaan energiavektori, jota on valmistettava primäärisestä polttoaineesta (mm. hiilivedyt, alkoholit, vesi) energiaa kuluttaen.

Perinteisesti vetyä valmistetaan maakaasun höyryreformointireaktiolla (SR), joka on endoterminen eli energiaa kuluttava reaktio. Helposti kuljetettavat ja varastoitavat nestemäiset polttoaineet soveltuisivat vedyn tai maakaasun sijasta paremmin mm. kulkuneuvojen polttokennojen polttoaineeksi. Koska SR:n reaktioentalpia kasvaa merkittävästi polttoaineen hiilivetyketjun kasvaessa, autoterminen reformointi (ATR), jossa yhdistyvät endoterminen SR ja eksoterminen osittaishapetus (POX), soveltuisi nestemäisten polttoaineiden prosessointiin SR:a paremmin.

Polttoaineiden aromaattiset jakeet ovat kemiallisesti vahvoja, minkä vuoksi ATR edellyttää korkeaa lämpötilaa (700–900 °C). Tällöin polttoaineen alifaattisten jakeiden termiset reaktiot kuitenkin voimistuvat tuottaen ei-toivottuja sivutuotteita ja lisäten koksin muodostusta katalyytin pinnalle. Riittävän aktiivisella, selektiivisellä ja kestävällä katalyytillä myös kaupallisten polttoaineiden reformointi voidaan suorittaa onnistuneesti.

Kaupallisten polttoaineiden ja niiden malliaineiden ATR:a tutkittiin jalometallikatalyyteillä (Rh, Pd, Pt) $ZrO_2$-kantajalla tavoitteena valmistaa vetyrikasta kaasuseosta, joka soveltuu kiinteäoksidipolttokennojen (SOFC) polttoainesyötöksi. Rh osoittautui aktiivisimmaksi SR:n suhteen, kun taas Pt oli aktiivisin hapetusreaktioissa. Bimetallisella RhPt-katalyytillä havaittiin Rh:n ja Pt:n olevan voimakkaassa vuorovaikutuksessa keskenään, mikä johti erittäin hyviin katalyyttisiin ominaisuuksiin ja mm. koksin muodostumisen vähenemiseen. Vähärikkisen dieselin ja sen malliaineiden ATR suoritettiin onnistuneesti RhPt-katalyyteillä. Nämä katalyytit osoittivat termistä kestävyyttä ja olivat lisäksi kestäviä heterosyklisten rikkiyhdisteiden suhteen.



Asiasanat vedyn valmistus, autoterminen reformointi, nestemäiset polttoaineet, jalometallikatalyytti, $ZrO_2$-kantaja

| ISBN (painettu) 978-951-22-9570-8 | ISSN (painettu) 1795-2239 |
|---|---|
| ISBN (pdf) 978-951-22-9571-5 | ISSN (pdf) 1795-4584 |
| Kieli englanti | Sivumäärä 71 s.+ liit. 41 s. |

Julkaisija Teknillinen korkeakoulu, Biotekniikan ja kemian tekniikan laitos

Painetun väitöskirjan jakelu Teknillinen korkeakoulu, Biotekniikan ja kemian tekniikan laitos

Luettavissa verkossa osoitteessa http://lib.tkk.fi/Diss/2008/isbn9789512295715/

## Preface

The practical work for this thesis was carried out in the Laboratory of Industrial Chemistry, Helsinki University of Technology, between January 2003 and September 2007. The work was part of projects FINSOFC 2002-2006 and SofcPower 2007-2011 financed by Tekes (The Finnish Funding Agency for Technology and Innovation). Funding from the Academy of Finland and the Ministry of Education through the Graduate School in Chemical Engineering (GSCE) is gratefully acknowledged. Kaute and Emil Aaltonen foundations and the Finnish Foundation for Technology Promotion (Tekniikan edistämissäätiö, TES) are thanked for personal grants.

I am most grateful to my supervisor, Professor Outi Krause, for her advice and support over the years of this study. Members of the FINSOFC 2002-2006 and SofcPower 2007-2011 projects at VTT, Wärtsilä Corporation and Neste Oil Corporation are thanked for their co-operation. I also wish to thank my colleagues at the Laboratory of Industrial Chemistry for providing a pleasant and motivating working atmosphere. Especially, I am indebted to my co-authors Andrea Gutiérrez, Satu Korhonen and Riku Slioor for fruitful discussions, to Johanna Hakonen for her co-operation in designing and constructing the reforming equipment, and to Kathleen Ahonen and Mary Metzler for revising the language of this overview and of the manuscripts.

Finally, I have my family and all friends to thank for their support. My warmest thanks go to Tuomas for his encouragement and to lovely Ronja for surrounding me with daily joy and laughter.

Espoo, September 2008

Reetta Kaila

## List of Publications

**This thesis consists of an overview and of the following appended publications, which are referred to in the text by their Roman numerals [I-V]:**

I R. K. Kaila and A. O. I. Krause, Steam reforming of heavy hydrocarbons, *Stud. Surf. Sci. Catal.* **147** (2004) 247-252.

II R. K. Kaila and A. O. I. Krause, Autothermal reforming of simulated gasoline and diesel fuels, *Int. J. Hydrogen Energy* **31** (2006) 1934-1941.

III R. K. Kaila, A. Gutiérrez, S. T. Korhonen and A. O. I. Krause, Autothermal reforming of *n*-dodecane, toluene, and their mixture on mono- and bimetallic noble metal zirconia catalysts, *Catal. Lett.* **115** (2007) 70-78.

IV R. K. Kaila, A. Gutiérrez, R. Slioor, M. Kemell, M. Leskelä and A. O. I. Krause, Zirconia-supported bimetallic RhPt catalysts: Characterization and testing in autothermal reforming of simulated gasoline, *Appl. Catal., B.* **84** (2008) 223-232.

V R. K. Kaila, A. Gutiérrez and A. O. I. Krause, Autothermal reforming of simulated and commercial diesel: The performance of zirconia-supported RhPt catalyst in the presence of sulfur, *Appl. Catal., B.* **84** (2008) 324-331.

**The author's contribution to the appended papers:**

I, II Reetta Kaila planned the research, calculated the thermodynamics, carried out the experiments, interpreted the results and wrote the manuscript.

III Reetta Kaila planned the research, prepared and characterised most of the catalysts, carried out most of the experiments, interpreted the results together with the co-authors and wrote the manuscript.

IV, V Reetta Kaila planned the research, prepared most of the catalysts, carried out most of the experiments, interpreted the characterisation results together with the co-authors and wrote the manuscript.

**Relevant to this thesis the following presentations have been given:**

I R. K. Kaila, A. Gutiérrez and A. O. I. Krause, Deactivation of RhPt/$ZrO_2$ catalysts in autothermal reforming of liquid fuels in the presence of sulfur, *poster*, 14th International Congress on Catalysis, Seoul, Korea, July 13–18, 2008.

II R. K. Kaila and A. O. I. Krause, Autothermal reforming of NExBTL on $ZrO_2$-supported RhPt catalysts, *poster*, Fuel Cell Annual Seminar, Espoo, Finland, March 12, 2008.

III R. K. Kaila, A. Gutiérrez and A. O. I. Krause, Autothermal reforming of commercial and simulated fuels in the presence of sulfur, *oral presentation*, Europacat VIII, Turku, Finland, August 26–31, 2007.

IV A. Gutierrez, R. K. Kaila and A. O. I. Krause, Autothermal reforming of simulated fuels on $ZrO_2$-supported bimetallic catalysts, *poster*, 12th Nordic Symposium on Catalysis, Trondheim, Norway, May 29–31, 2006.

V R. K. Kaila, M. K. Niemelä, K. J. Puolakka and A. O. I. Krause, Autothermal reforming of *n*-heptane and *n*-dodecane on nickel catalysts, *poster*, 11th Nordic Symposium on Catalysis, Oulu, Finland, May 23–25, 2004.

VI R. K. Kaila and A. O. I. Krause, Autothermal reforming of diesel fuel to hydrogen-rich fuel gas, *oral presentation*, 7th Natural Gas Conversion Symposium, Dalian, China, June 6–10, 2004.

VII R. K. Kaila and A. O. I. Krause, Steam and autothermal reforming of higher hydrocarbons, *poster*, 7th Natural Gas Conversion Symposium, Dalian, China, June 6–10, 2004.

# Nomenclature

## Abbreviations and symbols

| | |
|---|---|
| alumina | aluminium oxide ($Al_2O_3$) |
| APU | auxiliary power unit |
| ATR | autothermal reforming |
| BTL | biomass to liquid |
| cF4 | Pearson Symbol for a face-centred cubic (A1) crystal lattice structure |
| $CGH_2$ | compressed gaseous hydrogen |
| $d_i$ | inner diameter (mm) |
| $D$ | metal dispersion (%) |
| D | *n*-dodecane |
| 4,6-DMDBT | 4,6-dimethyldibenzothiophene |
| DR | dry reforming |
| DT | *n*-dodecane–toluene mixture |
| $D/T$ | dodecane to toluene ratio |
| $F_i$ | molar flow of compound i (mol/min) |
| fcc | face-centred cubic (crystals) |
| FC | flow control |
| FI | flow indication |
| FIC | flow indication and control |
| $\Delta G°$ | Gibbs free energy (kJ/mol) |
| GHG | greenhouse gases |
| $GHSV$ | gas hourly space velocity (1/h) |
| GTL | gas to liquid |
| H | *n*-heptane |
| $\Delta H°$ | reaction enthalpy (kJ/mol) |
| HDS | hydrodesulfurisation |

| | |
|---|---|
| HPLC | high performance liquid chromatography (pump) |
| IR | infrared |
| $LH_2$ | liquidised hydrogen |
| M, MCH | methylcyclohexane |
| $M_i$ | molar mass of compound i (g/mol) |
| MCFC | molten carbon fuel cell |
| MeOH | methanol |
| MHT | methylcyclohexane–*n*-heptane–toluene mixture |
| *M/H/T* | methylcyclohexane to *n*-heptane to toluene ratio |
| $n_i$ | concentration of compound i (mol%) |
| NG | natural gas |
| NSA | near surface alloy |
| OX | oxidation |
| PAFC | phosphoric acid fuel cell |
| PAH | polyaromatic hydrocarbon |
| PEMFC | polymer electrolyte membrane (a.k.a. proton exchange membrane) fuel cell |
| $P_i$ | concentration of product i (mol%) |
| PI | pressure indication |
| POX | partial oxidation |
| $r_F$ | average H/C molar ratio of the fuel (F) |
| SMSI | strong metal support interaction |
| SOFC | solid oxide fuel cell |
| SR | steam reforming |
| *St* | stoichiometric ratio of surface metal to adsorbed gas (mol/mol) |
| *T* | temperature (°C) |
| T | toluene |
| TI | temperature indication |
| TIC | temperature indication and control |
| *V* | volumetric flow ($cm^3$/min) |
| $V_m$ | molar gas volume, 22.41 l/mol at NTP |
| $V_i$ | irreversible uptake of adsorbed gas i ($ml/g_{cat}$) |

| | |
|---|---|
| WGS | water gas shift (reaction) |
| $x_F$ | average carbon number of the fuel (F) |
| $X_i$ | conversion of reactant i (mol%) |
| $Y_i$ | yield of compound i (mol/mol$C_{in}$) |
| zirconia | zirconium oxide ($ZrO_2$) |

### Subscripts

| | |
|---|---|
| i | compound i |
| C | carbon |
| F | fuel |
| M | metal |
| n | total number of compounds |
| NTP | normal temperature and pressure (0 °C, 1 bar) |
| tot | total |

### Characterisation tools

| | |
|---|---|
| BET | Brunauer–Emmett–Teller |
| DRIFT | diffuse reflectance Fourier transform infrared (spectroscopy) |
| EDX | energy dispersive X-ray |
| FID | flame ionisation detector |
| FT-IR | Fourier transform infrared (spectroscopy) |
| GC | gas chromatography |
| ICP-AES | inductively coupled plasma–atomic emission spectroscopy |
| MCT | mercury–cadmium–telluride (detector) |
| MS | mass spectrometer |
| SEM | scanning electron microscopy |
| TCD | thermal conductivity detector |
| TPR | temperature programmed reduction |
| XPS | X-ray photoelectron spectroscopy |
| XRD | X-ray diffraction |
| XRF | X-ray fluorescence |

# Autothermal reforming of simulated and commercial fuels on zirconia-supported mono- and bimetallic noble metal catalysts

# 1 Introduction

Energy consumption continues to climb as world population grows and the standard of living rises. Meanwhile world oil resources are diminishing. New energy sources are acutely needed to keep the energy supply and demand in balance. At the same time, the level of emissions and exhaust gases needs to be reduced to minimise their contribution to the greenhouse effect. In the long run, global warming might bring with it natural catastrophes such as floods, droughts and hurricanes all over the world. Understandably, renewable energy sources – biomass, wind and solar energy – as well as hydrogen ($H_2$) are attracting close attention, and more efficient technologies for energy recovery are being sought. One promising highly efficient technology is fuel cells running on hydrogen. Indeed, the substitution of the fuel cell for the combustion engine is a powerful option for reducing greenhouse gas (GHG) emissions to the atmosphere, in particular $CO_2$.

The major advantages of using hydrogen (or $H_2$-rich mixtures, e.g., synthesis gas) as fuel include the clean combustion, the possibility of long-term storage of the primary fuel and the diversity of primary fuels (natural gas (NG), biomass, crude oil) that can be used in the production [1,2]. Hydrogen is conventionally produced by steam reforming of NG. The growing use of fuel cell technologies in heat and power production, as replacements for internal combustion engines and as auxiliary power units (APUs) in mobile applications will vastly increase the demand for hydrogen production [3,4]. Certainly the development of an economy based on hydrogen would require major structural changes that could take several decades. In the meantime, commercially

available fuels such as gasoline and diesel could be used as hydrogen carriers to achieve immediate reductions in GHG emissions [1]. Liquid fuels also have the advantages that they are easy to deliver and safe to store and the infrastructure is already in place. [5 - 7]

## 1.1 Fuel cells

Fuel cell applications for energy production have been investigated extensively in the last decade owing to their high energy efficiency. Not only does the high energy efficiency as such achieve reductions in $CO_2$ emissions, but also the exhaust levels ($CO_x$, $NO_x$ and $SO_x$) are lower than for combustion engines [8].

There are several types of fuel cells available, which can be utilised in applications from laptops to fuel cell-powered vehicles and stationary energy production units [9]. The applications and their needs and limitations affect the choice of fuel cell type, as well as the fuel utilised in the fuel cell process [5]. Phosphoric acid fuel cells (PAFCs), molten carbon fuel cells (MCFCs) and solid oxide fuel cells (SOFCs) are designed for centralised energy production, where the system has to be stable but volume and weight restrictions are not set. Polymer electrolyte membrane fuel cells (PEMFCs), on the other hand, are designed for smaller scale use and their operating temperature is low (Table 1). Because of the low temperature, the catalytic material (Pt) of the PEMFC does not tolerate carbon monoxide. Thus, pure hydrogen and methanol (MeOH) are the most suitable fuels for PEMFC. [9]

Table 1. Fuel cell characteristics [10].

| Fuel cell type | Cell temperature (°C) | Maximum CO content (ppm) | Fuel |
|---|---|---|---|
| PEMFC | 70-80 | 50 | $H_2$, MeOH |
| PAFC | 200 | 500 | $H_2$ |
| MCFC | 600-650 | No limit | $H_2$, $CH_4$, CO, MeOH |
| SOFC | 700-1000 | No limit | $H_2$, $CH_4$, CO, MeOH |

High temperature fuel cells (MCFC and SOFC) are capable of converting methane, carbon monoxide and alcohols in the anode chamber by internal reforming [11]. That is, alongside the exothermic oxidation reactions of the fuel cell, either direct or indirect endothermic reforming of methane is carried out. The temperature of the fuel cell is thereby controlled and the heat losses are minimised. Methane is, thus, a desired component of the reformate. The exhaust gas of high temperature fuel cells consists of steam and carbon dioxide. A scheme of the SOFC system is presented in Figure 1.

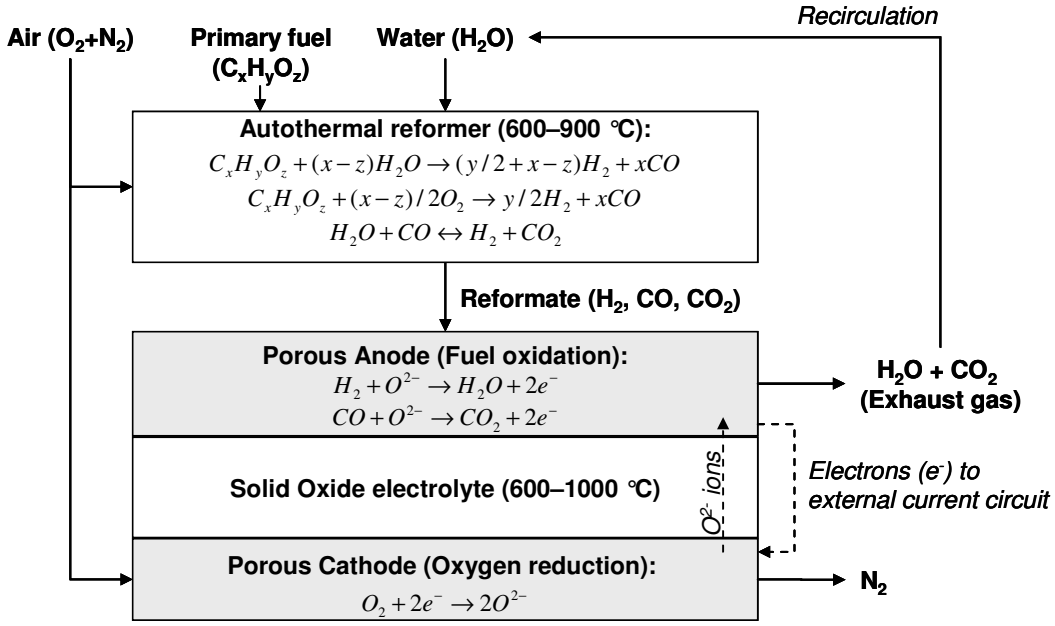


Figure 1. Scheme of a SOFC combined with an on-board reformer [12].

In mobile applications, the alternative fuels for fuel cells are MeOH and commercial fuels, such as gasoline and diesel, which today can easily be delivered and stored. In stationary energy production, in the vicinity of NG pipe lines, on the other hand, NG and propane are reasonable choices for fuels. Biofuels such as ethanol and biodiesel (e.g., second generation biodiesel, biomass to liquid (BTL) fuels) are also feasible in local applications, especially now that sustainable development ($CO_2$ neutrality) is an issue. All these compounds ($C_xH_yO_z$) must, however, be reformed to $H_2$-rich reformate for use in a SOFC (Figure 1). [3,6]

## 1.2 Reforming of liquid fuels

Hydrogen as such is not available in the environment, and it has to be produced from hydrogen-containing compounds (water ($H_2O$), hydrocarbons ($C_xH_y$), alcohols ($C_xH_yO_z$)). Since, the production of hydrogen consumes energy, hydrogen is not properly an energy source but an energy carrier, or vector.

Hydrogen and synthesis gas ($H_2 + CO$) are widely produced by steam reforming (SR) of NG in stationary systems:

$$CH_4 + H_2O \Leftrightarrow 3H_2 + CO \qquad \Delta H°_{298} = 206.2\ kJ/mol \qquad (1)$$

Although both are easily utilised in the vicinity of NG pipelines, they must be compressed when transported or stored in vehicles. Liquid hydrocarbons then become a good alternative (Table 2). Diesel, in particular, has a very high volumetric $H_2$ density [13].

Table 2. Volumetric $H_2$ density of fuels and the SR enthalpy at 700 ºC for $H_2$ production [14].

| **Fuel** | | **Volumetric $H_2$ density** | **Enthalpy of SR $\Delta H_{700\ °C}$** | |
|---|---|---|---|---|
| | | kmol/50 $dm^3_{Fuel}$ | $kJ/mol_{Fuel}$ | $kJ/mol_{H2}$ |
| **Hydrogen** | *gas, 700 bar* ($CGH_2$) | 1.4 | - | - |
| | *liquid, -253 °C* ($LH_2$) | 1.7 | | |
| **Fossil fuels** | Natural gas (NG) *gas, 700 bar* | 3.2 | 224 | 75 |
| | *liquid, -162 °C* | 3.5 | | |
| | Gasoline ($C_7H_{14}$) | 2.6 | 1140 | 81 |
| | Diesel ($C_{16}H_{34}$) | 3.2 | 2806 | 85 |
| **Renewable fuels** | Methanol | 2.5 | 105 | 52 |
| | Ethanol | 2.6 | 163 | 41 |
| | 2nd generation biodiesel (BTL, $C_{16}H_{34}$) | 3.2 | 2806 | 85 |
| | Water | 2.8 | - | -* |

* Electrolysis: $H_2O = H_2 + ½\ O_2$, $\Delta G° = 237\ kJ/mol_{H2}$.

*$CGH_2$ = compressed gaseous hydrogen*

*$LH_2$ = liquidised hydrogen*

Hydrogen can be produced from liquid hydrocarbons by various technologies, not only SR (Eq. 2) but also partial oxidation (POX, Eq. 3), dry reforming (DR, Eq. 4, also known as $CO_2$ reforming) and combinations of these [1,4].

$$C_xH_y + xH_2O \Leftrightarrow \left(\frac{y}{2} + x\right)H_2 + xCO \quad (SR) \tag{2}$$

$$C_xH_y + \frac{x}{2}O_2 \Leftrightarrow \frac{y}{2}H_2 + xCO \quad (POX) \tag{3}$$

$$C_xH_y + xCO_2 \Leftrightarrow \frac{y}{2}H_2 + 2xCO \quad (DR) \tag{4}$$

SR gives a high yield of $H_2$, but energy requirements are large due to the endothermic nature of the reaction [15,16]. SR of "high molecular weight hydrocarbons" (i.e., light distillate naphtha) is a large-scale commercial process, which has been practiced for the last 40 years in locations where NG is not available [17,18]. DR is even more endothermic than SR and gives a lower $H_2$/CO ratio for the product [1]. A lower $H_2$/CO ratio is also obtained in POX; however, POX is an exothermic process and may require external cooling [15].

The combination of SR and POX is known as autothermal reforming (ATR). The hydrocarbons react with $H_2O$ and $O_2$ in a process where high energy efficiencies are achieved since the exothermic POX reaction provides the heat needed for the endothermic SR reaction [15]. The process is simple in design and the required monetary investment is low [16]. In the presence of oxygen, however, complete oxidation (OX) is possible (Eq. 5). Also, the water gas shift reaction (WGS, Eq. 6) takes place in ATR [16], and the reaction equilibrium can be shifted through changes in operating conditions, such as reaction temperature and the amount of steam. Besides being catalysed by conventional Cu-based catalysts, the WGS reaction is catalysed by noble metals [19,20]. At operating temperatures below 815 °C, the WGS reaction equilibrium shifts from $H_2O + CO$ to $H_2 + CO_2$.

$$C_xH_y + \left(\frac{y}{2} + x\right)O_2 \Leftrightarrow \frac{y}{2}H_2O + xCO_2 \quad (OX) \tag{5}$$

$$H_2O + CO \Leftrightarrow H_2 + CO_2 \quad (WGS) \qquad \Delta H°_{298} = \text{-41.1 kJ/mol} \tag{6}$$

ATR is the preferred choice for mobile applications (e.g., in ships) because of its greater thermal stability than SR [8], the short start-up time [21] and the lower volume and weight [22]. The ATR reformate, containing mainly $H_2$, CO, $CO_2$, $CH_4$ and $H_2O$, is also an optimal feedstock for SOFC although the selectivity for hydrogen is lower in ATR than in SR [23].

## 1.3 Challenges in reforming of liquid hydrocarbon fuels

One of the major problems encountered with the conventional Ni-based catalyst is the deactivation due to carbon deposition (Eqs. 7–10). In the reforming of liquid fuels the presence of aromatic hydrocarbons increases the risk of carbon deposition [10,11,24]. Possible coke forming reactions are listed below [17,18]:

$$C_xH_y \Leftrightarrow mH_2 + C_{x-m}H_{y-2m} + mC_{(s)} \tag{7}$$

$$2CO \Leftrightarrow CO_2 + C_{(s)} \quad \text{(Boudouard reaction)} \quad \Delta H°_{298} = \text{-172.4 kJ/mol} \tag{8}$$

$$CO + H_2 \Leftrightarrow H_2O + C_{(s)} \qquad \Delta H°_{298} = \text{-131.3 kJ/mol} \tag{9}$$

$$CH_4 \Leftrightarrow 2H_2 + C_{(s)} \qquad \Delta H°_{298} = \text{74.6 kJ/mol} \tag{10}$$

The nickel catalysts are also highly sensitive to the sulfur present in commercial fuels [17,24,25]. Although most sulfur compounds can be removed by the present catalytic hydrodesulfurisation (HDS) technology, certain heterocyclic compounds are difficult

and expensive to remove [26,27]. Thus, “sulfur-free” fuels in fact contain traces of sulfur compounds (< 10 ppm S) even after the HDS treatment. Of particular note are the dialkyldibenzothiophenes, of which 4,6-dimethyldibenzothiophene (4,6-DMDBT) is the most stable [26,28]. The high resistance of 4,6-DMDBT to HDS processes is proposed to be due to the steric hindrance of the methyl groups (Figure 2), which prevent contact between the thiophenic sulfur atom and the active site of the catalyst [26,29]. The problems due to sulfur can be overcome by using sulfur-free fuels, as, for example, Fischer-Tropsch diesel (gas to liquid (GTL) or BTL), but such fuels are not yet widely available. An alternative approach is to use more stable catalysts with conventional fuels. The effect of sulfur on the reforming of liquid hydrocarbons has gained considerable attention, but relatively little information is available in the literature, as noted in the recent review by Shekhawat et al. [30].

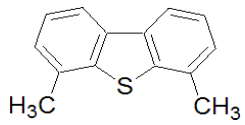


Figure 2. Molecular structure of 4,6-dimethyldibenzothiophene (4,6-DMDBT).

## 1.4 $ZrO_2$-supported noble metal catalysts

In reforming reactions, noble metal catalysts are superior to nickel catalysts in their tolerance of sulfur [7,31 - 33] and resistance to coke deposition [7,24,31,34 - 36]. Moreover, the addition of a second metal such as Pt, Pd or Rh [3,34,37] to the nickel catalyst improves the catalyst stability. Rhodium in particular has shown high resistance to sulfur poisoning and carbon deposition, yielding high conversions of hydrocarbons and high selectivity for hydrogen [3].

Noble metals, especially Rh, are also noted for their activity in reforming of hydrocarbons [7], and higher activity enables a lower metal loading than in the conventional catalyst (e.g., 15 wt% $NiO/Al_2O_3$). Indeed, low noble metal loadings are essential since noble metals (Figure 3) are more expensive than Ni (US$ 28.5/kg in April 2008) [38]. It bears notice that especially the price of rhodium has risen ten-fold

over the past three years (Figure 3) [39]. Also the catalyst lifetime is playing an important role.

Despite their cost, noble metal catalysts are already widely applied in catalytic converters for automobile exhaust gases, where bimetallic RhPt catalysts play a crucial role in the simultaneous oxidation (Pt) of hydrocarbons and CO and reduction of $NO_x$. Extensive research has, thus, been carried out on these so-called three-way catalysts [40 - 43]. However, the behaviour of RhPt catalysts has mainly been studied on a theoretical level, using flat, single-crystal metal samples [43 - 46]. The presence of a Rh-Pt alloy is considered a certainty [41]. Indeed, the superiority of bimetallic RhPt catalysts to the corresponding monometallic catalysts suggests a synergism between the two metals [47] and the formation of an alloy [48,49].

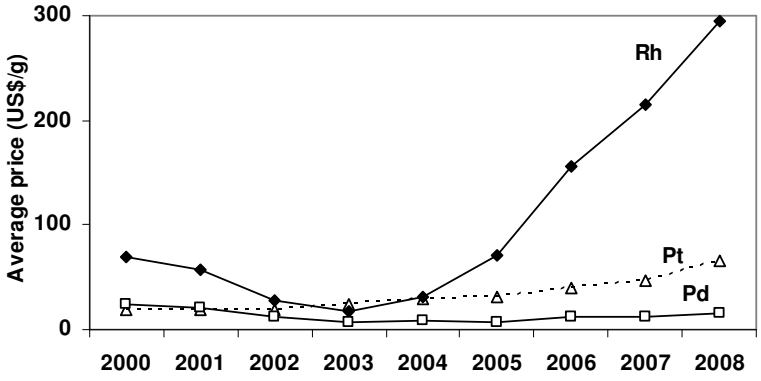


Figure 3. Price development of Rh, Pt and Pd since year 2000 [39].

The material used as the catalyst support also affects the catalyst performance [20,37,50,51]. Industrial reforming catalysts are conventionally supported on α-alumina (α-$Al_2O_3$) or modified $Al_2O_3$ (e.g., combination with MgO) [24]. However, $ZrO_2$ is the preferred support for Rh catalysts in order to avoid the detrimental interaction between Rh and $Al_2O_3$, which reduces the activity of the catalyst [35]. $ZrO_2$ is also noted for its stability [52]. As an acid–base bifunctional oxide, $ZrO_2$ is less acidic than $Al_2O_3$ [53,54], which means reduced thermal cracking reactions and coke formation [55]. The lower acidity of $ZrO_2$ also increases the tolerance to sulfur [56]. Thus, the use of $ZrO_2$ as a support is promising. Despite its good features, $ZrO_2$ has thus far enjoyed only limited use as a support owing to its low surface area [50,53,55].

## 1.5 Scope of the research

The use of low-sulfur diesel and other commercial hydrocarbon fuels as primary fuel for SOFC systems was investigated. The advantage of diesel as primary fuel is its high volumetric $H_2$ density and the existing infrastructure. Liquid fuels are easy to deliver and store and particularly attractive for mobile and local applications [6,7]. Before it can be utilised in the fuel cell, the primary fuel must be converted into $H_2$-rich fuel gas (i.e., synthesis gas). The reforming of hydrocarbons is a catalytic reaction requiring high temperatures. Moreover, the risk of undesired side reactions (i.e., thermal cracking), carbon deposition and sulfur poisoning of catalysts increases when the hydrocarbons are commercial fuels.

This work concerns the ATR of simulated fuels and low-sulfur diesel on mono- and bimetallic noble metal catalysts. Conventionally hydrogen is produced by SR of NG on Ni-based catalysts [24]. With liquid fuels, however, SR becomes highly endothermic, whereas ATR can be operated under thermoneutral conditions. SR and ATR of hydrocarbon model compounds were compared (Paper I), and the reforming conditions were optimised to suppress the coke accumulation and thermal cracking reactions. *n*-Heptane and *n*-dodecane were used as model compounds for the *n*-alkane fractions of gasoline and diesel, respectively, and toluene and methylcyclohexane as model compounds for the aromatic and cycloalkane fractions (Paper II).

In the ATR experiments the conventional nickel catalyst was replaced with $ZrO_2$-supported mono- (Rh, Pd, Pt) and bimetallic (RhPt) noble metal catalysts, which tolerate sulfur and do not promote coke formation [31]. The metal loading was kept low (0.5 wt%) since otherwise they would not be economically viable (Papers III and IV).

Simulated fuels containing 4,6-DMDBT or $H_2S$ as the sulfur compound ($S < 10$ ppm), were evaluated as models for commercial low-sulfur diesel. The effect of sulfur on the performance of the noble metal catalyst and the coke deposition was examined, and the roles of Rh and Pt in the bimetallic RhPt catalysts were studied (Papers IV and V).

# 2 Materials and methods

$ZrO_2$-supported noble metal catalysts (Rh, Pd, Pt) were prepared and their performance in reforming of simulated and commercial fuels was evaluated and compared with the performance of commercial 15 wt% $NiO/Al_2O_3$. All gases and chemicals used in the catalyst preparation, characterisation and testing are listed in Table 3.

## 2.1 Catalyst preparation

$ZrO_2$-supported mono- (Rh, Pd, Pt) and bimetallic (RhPt) catalysts were prepared by dry impregnation and dry co-impregnation from nitrate (Rh, Pd, Pt), ammonium nitrate (Pt) and chloride (Pt) solutions to give not more than 0.5% noble metal by weight.

The $ZrO_2$ support (MEL Chemicals EC0100) was ground to a particle size of 0.25–0.42 mm and calcined at 900 °C for 16 hours. After impregnation the catalysts were dried at room temperature for 4 hours and at 100 °C overnight. Finally, the catalysts were calcined at 700 or 900 °C for 1 hour. This preparation procedure is described in detail in Papers III & IV.

The mono- and bimetallic catalysts were designated Rh, Pd, Pt, 0.5RhPt, 1RhPt and 2RhPt, where the numbers 0.5, 1 and 2 correspond to the intended *Rh/Pt* molar ratio of the bimetallic catalysts. The calcination temperature is reported in parentheses: (700) or (900).

Table 3. Gases and chemicals used in catalyst preparation, characterisation and testing in reforming reactions of liquid hydrocarbons.

| Gases and chemicals | Use | Supplier | Purity | Paper |
|---|---|---|---|---|
| Hydrogen ($H_2$) | Pretreatment, TPR, DRIFTS, chemisorption | Aga | 99.999 % | I, III, IV |
| Argon (Ar) | Inert, TPR | Aga | 99.999 % | I - V |
| $H_2$ in Ar | TPR | Aga | 99.999 % | IV |
| 20% Oxygen ($O_2$) in Helium (He) | TPR | Aga | 99.996 % | IV |
| Carbon monoxide (CO) | DRIFTS, chemisorption | Messer Griesheim | 99.997 % | III - IV |
| Nitrogen ($N_2$) | Inert, physisorption | Aga | 99.999 % | I - V |
| Synthetic air, 20% $O_2$ in $N_2$ | Reactant | Aga | 99.99 % | I - V |
| 10% $O_2$ in $N_2$ | DRIFTS | Aga | 99.99 % | III-IV |
| $H_2S$ in $N_2$ | Additive | Aga | 0.5 % | V |
| $Rh(NO_3)_3$ in nitric acid (5 wt%) | Precursor | Sigma-Aldrich | 10 % | II - V |
| $Pt(NH_4)_4(NO_3)_2$ | Precursor | Strem Chemicals | 99 % | II - III |
| $Pt(NH_3)_2(NO_2)_2$ | Precursor | Aldrich | 3.4 % | IV - V |
| $Pt(NO_3)_4$ | Precursor | Johnson-Matthey | 16 % | III |
| $H_2(PtCl_6)$ | Precursor | Merck | 3.8 % | III |
| $Pd(NO_3)_2$ | Precursor | Alfa-Aesar | 8.5 % | III |
| 15% $NiO/Al_2O_3$ | Catalyst | BASF | | I - II |
| $ZrO_2$ (EC0100) | Support | MEL Chemicals | | II - V |
| *n*-Heptane | Reactant | Fluka | ≥ 99.5% | I - II |
| | | Sigma-Aldrich | 99 % | IV - V |
| *n*-Dodecane | Reactant | Sigma-Aldrich | 99+ % | II - III, V |
| Toluene | Reactant | Riedel-de Haën | ≥ 99.7% | II - V |
| Methylcyclohexane | Reactant | Merck | ≥ 99% | II |
| | | Fluka | ≥ 99.5% | IV - V |
| Low-sulfur diesel | Reactant | Neste Oil | | V |
| 4,6-DMDBT | Additive | Aldrich | 97 % | V |

## 2.2 Catalyst characterisation

The noble metal loadings of the fresh and used catalysts were determined by inductively coupled plasma–atomic emission spectroscopy (ICP-AES) (Papers III and IV). For comparative purposes, the metal loadings of the fresh catalysts were measured with an X-ray fluorescence spectrometer (XRF) equipped with UniQuant 4 software (Paper IV).

The chemical and physical properties of the catalysts were characterised by chemisorption ($H_2$ and CO uptakes) (Papers III and IV), physisorption (BET surface area, total pore volume) (Paper IV) and *in situ* diffuse reflectance Fourier transform infrared spectroscopy (DRIFTS) (Papers III and IV).

XRD, XPS, $H_2$-TPR, SEM and EDX were used to study the composition and morphology of the catalyst surface (Paper IV) of selected mono- (Rh, Pt) and bimetallic (2RhPt) catalysts. The low metal loading of the catalysts affected the accuracy of the catalyst characterisation.

## 2.3 Reforming of liquid hydrocarbons

SR and ATR were performed with the equipment presented in Figure 4. The feed consisted of *n*-heptane (H), *n*-dodecane (D), toluene (T), methylcyclohexane (M), mixtures of these hydrocarbons (simulated fuels) or low-sulfur diesel, plus water and air. The catalyst bed (0.05–0.3 g) was placed in the middle of the tubular quartz reactor ($d_i$ = 10 mm). The hydrocarbons and water were vaporised and mixed with air before introduction to the reactor (see Figure 4), and the inlet temperature (400–900 ºC) was controlled with a three-zone furnace. The total flow rate of the reactants was 100–300 $cm^3/min_{NTP}$, and the feed was diluted with argon to a total flow rate of 300–900 $cm^3/min_{NTP}$. The gas hourly space velocity (*GHSV*) was $1.6 \cdot 10^5$–$1.4 \cdot 10^6$ 1/h. The $H_2O/C$ and $O_2/C$ feed ratios of the ATR experiments were set to 2.3–5 mol/mol and 0–0.34 mol/mol, respectively.

In the preliminary experiments (Paper I), SR and ATR reactions of *n*-heptane were compared on a commercial 15 wt% $NiO/Al_2O_3$ catalyst (0.2–0.3 mm) at 500–725 °C to choose the appropriate process for $H_2$ production from commercial fuels. The

experimental procedure is described in detail in Paper I. The reaction conditions for ATR were optimised, and ATR of the simulated fuels was then studied on noble metal catalysts (Rh, Pd, Pt) (Papers II and III). For comparison, ATR experiments were also performed on 15 wt% $NiO/Al_2O_3$ (Paper II) and $ZrO_2$ (Papers III and IV) and in the absence of catalyst or support (thermal cracking) (Papers II and IV).

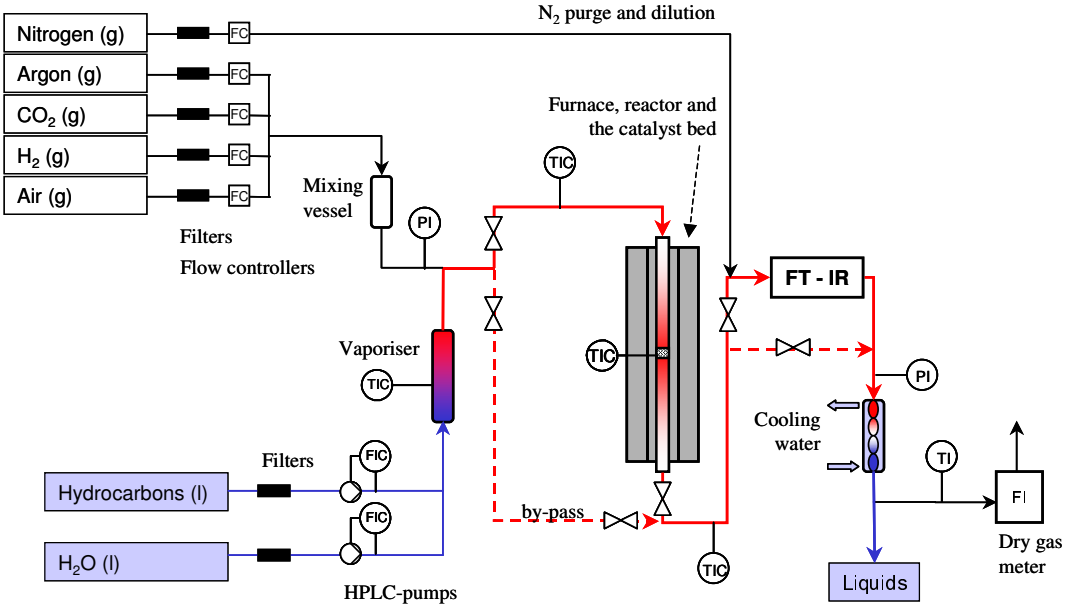


Figure 4. Equipment for reforming of liquid hydrocarbons.

The sulfur tolerance of $ZrO_2$-supported mono- and bimetallic RhPt catalysts was studied in ATR of commercial fuels and of simulated fuels in the presence of a sulfur compound ($H_2S$ or 4,6-DMDBT) to give 10 ppm of S in fuel (Paper V). The simulated fuel consisted of the DT or MHT mixture with the molar ratios *D/T* = 80/20 and *M/H/T* = 50/30/20, respectively. The commercial low-sulfur diesel (< 10 ppm S) with aromatic content of 17.4 wt% was provided by Neste Oil Corporation. The density of the diesel was measured to be 0.824 g/cm$^3$. The experiments with sulfur were performed at VTT (Technical Research Centre of Finland) with similar equipment to that presented in Figure 4. In these experiments the catalyst amount was 0.2 g. The flow rates of the liquid fuel and water to the reactor were 0.038 g/min and 0.149 g/min, respectively. The total flow rate of the reactants, including oxygen, was 300 cm$^3$/min$_{NTP}$, and the flow

was diluted with nitrogen to give a total flow rate of 900 $cm^3/min_{NTP}$ ($GHSV = 3.1 \cdot 10^5$ 1/h). The $H_2O/C$ and $O_2/C$ molar ratios were 3 mol/mol and 0.34 mol/mol, respectively.

After every experiment, the reactor was flushed with Ar or $N_2$ and cooled down to room temperature. The amounts of carbon and sulfur in the fresh and used catalysts were determined with a Leco SC-444, where the sample was burnt with oxygen at 1350 °C (Papers III and V).

## 2.4 Product analysis and definitions

In the preliminary experiments, the product flow from SR and ATR of *n*-heptane was analysed with two online gas chromatographs (GC, Hewlett-Packard, HP 5890) with a sampling frequency of 40 minutes. The hydrocarbons were separated in a DB-1 column and detected with FID on one GC, and $H_2$, $O_2$, $N_2$, Ar, CO, $CO_2$, $CH_4$ and $H_2O$ were separated in a packed column (activated carbon with 2% squalane) and detected with TCD on the other. (Paper I) Each analysis was followed by a back-flush sequence performed for the packed column.

In all subsequent experiments, the feed and product flows were diluted with $N_2$ (900 $cm^3/min_{NTP}$) and analysed with an on-line Fourier transform infrared (FT-IR) spectrometer (Gasmet$^{TM}$) equipped with a Peltier-cooled mercury–cadmium–telluride (MCT) detector and multicomponent analysis software (Calcmet) [57]. When IR radiation (600–4200 $cm^{-1}$) is transmitted through the gas sample, certain wavelengths of the radiation are absorbed by the gas molecules, with the exception of diatomic homonuclear gases (e.g., $N_2$, $H_2$, $O_2$) and noble gases (e.g., He, Ar), which do not absorb radiation and cannot be analysed. A sample spectrum produced by multicomponent analysis is presented in Figure 5.

With FT-IR, the composition of the flow can be followed in 1 s to 3 min. The sample cell was kept at 230 ºC to avoid condensation of the fed hydrocarbons and water. The compounds analysed were $H_2O$, CO, $CO_2$, $CH_4$, $C_2H_2$, $C_2$–$C_5$ alkenes, $C_2$–$C_7$ alkanes, $C_1$–$C_4$ alcohols, benzene, toluene, cyclohexane and methylcyclohexane. The lowest detectable concentrations were 0.5–3 ppm and the accuracy of the analysis was 2%.

After the analysis the flows were condensed and the dry gas flow was measured (see Figure 4).

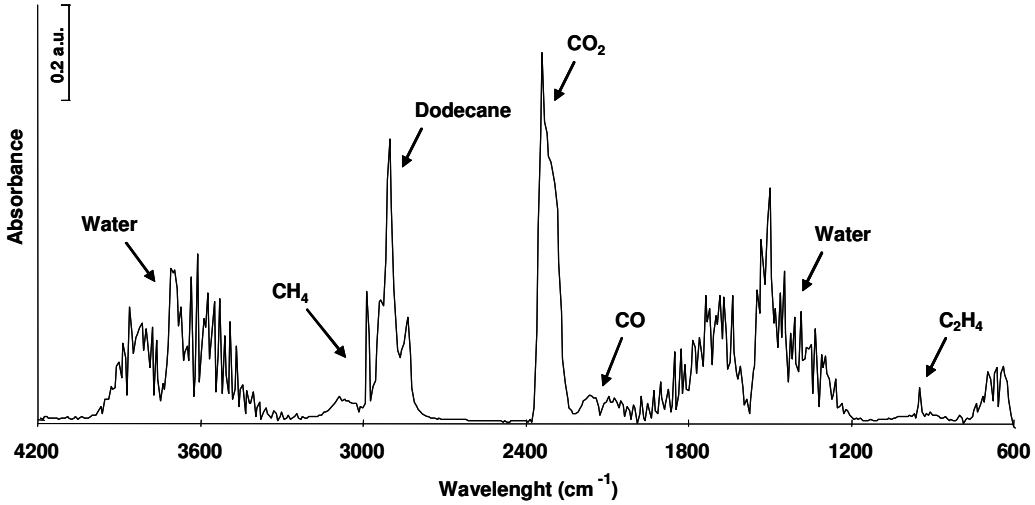


Figure 5. Sample spectrum obtained with a multicomponent FT-IR analyser.

In the experiments with sulfur, the water and the higher hydrocarbons in the product were condensed before the analysis, and the dry gas flow ($H_2$, CO, $CO_2$, $CH_4$ and $O_2$) was analysed with an extractive gas analyser (S 710, Sick Maihak Inc.) operating at 0–45 ºC. Dräger ampoules capable of detecting $H_2S$ in amounts from 0.5 to 15 ppm were used to determine the presence of $H_2S$ in the wet and dry flows. In the presence of $H_2S$, the color of the Dräger-ampoule changes from white to light brown (HgS) due to the following reaction:

$$H_2S + Hg^{2+} \Leftrightarrow HgS + 2H^+ \qquad (11)$$

The conversions ($X_i$, mol%) of the hydrocarbons and water were calculated from the feed and product flows ($F_i$, mol/min) (Eq. 12). The weighted averages for the hydrocarbon conversions of the mixtures were calculated to determine the overall hydrocarbon conversion (Eq. 13).

$$X_i = \frac{F_{i,in} - F_{i,out}}{F_{i,in}} \cdot 100\% \quad (12)$$

$$X_{tot} = \sum (n_{i,in} \cdot X_i) \quad (13)$$

The element balances and the amounts of hydrogen produced and oxygen consumed were determined from the analysed product distribution and the measured dry gas flow. The product distribution was calculated with Eq. 14, and the yield of compound i ($Y_i$, mol/mol $C_{in}$) was defined as the ratio of the molar flow of product i to the amount of carbon in the hydrocarbon feed flow (Eq. 15):

$$P_i = \frac{F_i}{\sum_{n=1}^{j} F_n} \cdot 100\% \quad (14)$$

$$Y_i = \frac{F_i}{F_{C\,in}} \quad (15)$$

In the experiments performed at VTT, the conversion of oxygen was calculated from the analysed feed and product flows ($F_i$) (Eq. 12), and the conversions of the simulated and commercial fuels ($X_F$) and water ($X_{H2O}$) were calculated from the molar feed flows and the amounts of $H_2$, CO, $CO_2$ and $CH_4$ that were produced (Eqs. 16 and 17).

$$X_F = \frac{(F_{CO,out} + F_{CO_2,out} + F_{CH_4,out}) / x_F}{F_{F,in}} \cdot 100\%\,, \quad (16)$$

$$X_{H_2O} = \frac{(2 \cdot F_{H_2,out} + 4 \cdot F_{CH_4,out} - r_F \cdot x_F \cdot X_F \cdot F_{F,in})}{2 \cdot F_{H_2O,in}} \cdot 100\%\,, \quad (17)$$

where $x_F$ is the average carbon number and $r_F$ the average H/C molar ratio of the fuel (F): $x_{diesel}$ = 16 and $r_{diesel}$ = 1.9, $x_{DT}$ = 11 and $r_{DT}$ = 2.0 and $x_{MHT}$ = 7 and $r_{MHT}$ = 1.9. The accuracy of these calculations was estimated from the error of the oxygen balance (Eq. 18):

$$error = \frac{(2 \cdot F_{O_2,in} - (F_{CO,out} + 2 \cdot F_{CO_2,out} + 2 \cdot F_{O_2,out} + (1 - X_{H_2O}) \cdot F_{H_2O,in}))}{2 \cdot F_{O_2,in}} \cdot 100\% \qquad (18)$$

Catalyst selectivity for the reforming reactions (SR, POX and DR) is presented as the reforming to oxidation molar ratio (*Ref/Ox*, Eq. 19), which is calculated from the product distribution. Hydrogen in formed not only in the reforming reactions but also by the WGS equilibrium reaction (Eq. 6), thus the production of hydrogen does not directly reveal the catalyst selectivity for reforming. However, when considering the *Ref/Ox* molar ratio, the effect of WGS reaction is eliminated, because in spite of the WGS reaction the sums of $H_2$+CO and $H_2O$+$CO_2$ remain equal (Paper IV).

$$Ref/Ox = \frac{P_{H_2} + P_{CO}}{P_{H_2O} + P_{CO_2}} \qquad (19)$$

## 2.5 Thermodynamics

Thermodynamics for ATR reactions (Eqs. 2–4) of the hydrocarbons (*n*-heptane, *n*-dodecane, toluene and methylcyclohexane) and their mixtures were preformed with HSC Chemistry version 5.11 [14]. The effects of side reactions such as the WGS (Eq. 6), thermal cracking and carbon formation reactions (Eqs. 7–10) were included. Also hydrogenation and dehydrocyclisation reactions of the $C_7$ hydrocarbons in the MHT mixture were studied. (Paper II)

The oxidation of the metals (Ni, Rh, Pd, Pt) on the catalysts as well as the possibility of the formation of volatile Rh and Pt species (from the bulk phase) under ATR conditions was investigated in the temperature range of 0–1500 °C.

# 3 Optimisation of reaction conditions

The reactions conditions for the production of $H_2$-rich fuel gas from liquid hydrocarbon fuels were optimised based on thermodynamic calculations and experimentally, by varying the operation conditions. Hydrocarbon fuels were simulated with various model compounds and their mixtures, *n*-heptane and *n*-dodecane being the model compounds for aliphatic fractions of commercial fuels, and toluene and methylcyclohexane for aromatic and cycloalkane fractions, respectively.

## 3.1 Thermodynamics

Hydrogen is conventionally produced by SR (Eq. 1) of NG, which is an endothermic reaction. The value of SR reaction enthalpy increases noticeably with the chain length of the hydrocarbon, and with liquid hydrocarbons as hydrogen source the reaction enthalpy becomes as much as ten-fold that of pure methane (see Table 2). However, when oxygen is added (ATR), the total system can be driven to thermoneutral conditions, and ATR becomes an interesting alternative to SR.

According to thermodynamics, the highest hydrogen selectivity in SR of the model hydrocarbons is achieved at approx. 700 °C (see Figure 6 for *n*-heptane). Methanation and coke formation can occur at lower temperatures, whereas light hydrocarbons are formed at higher temperatures.

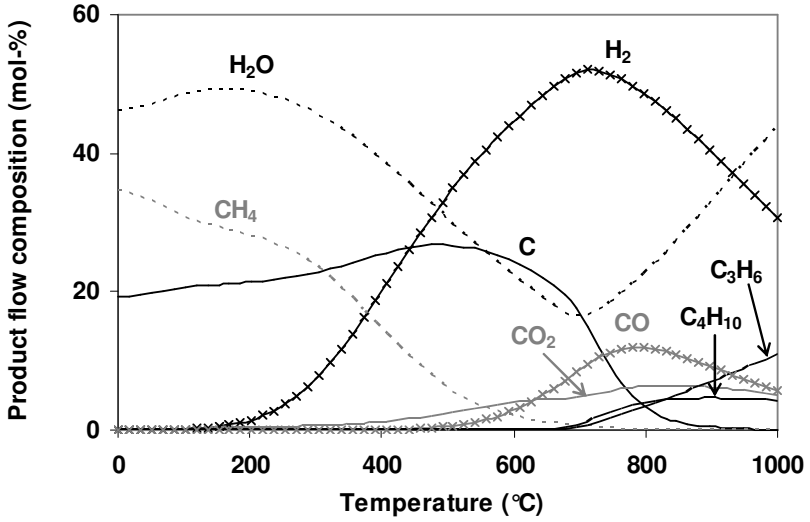


Figure 6. Thermodynamic product distribution for SR of *n*-heptane ($H_2O/C$ = 1 mol/mol).

The suggested flow scheme for the main and side reactions present in the autothermal reformer is depicted in Figure 7.

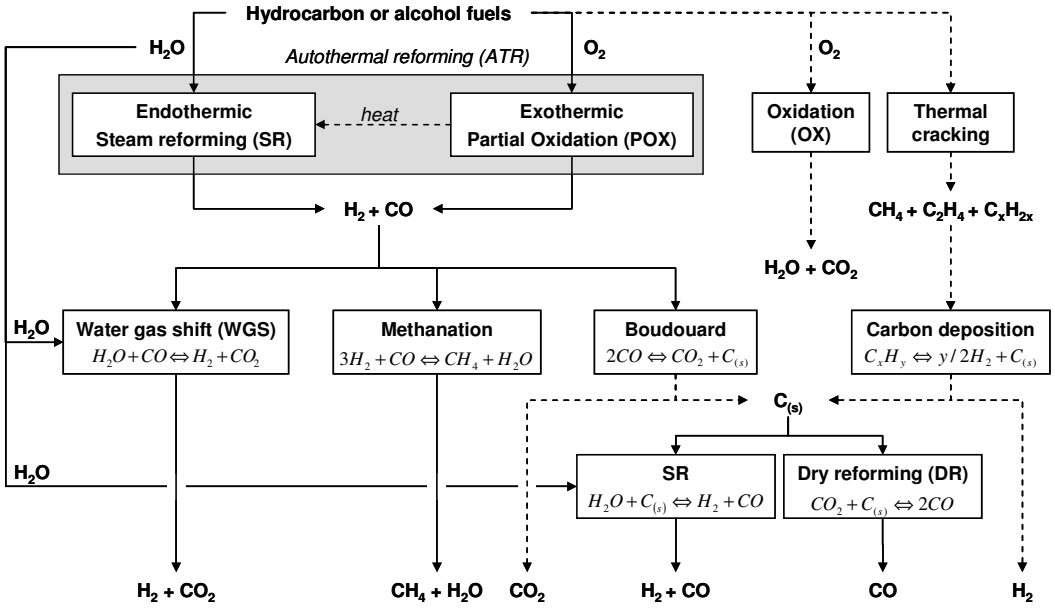


Figure 7. Flow scheme of possible reactions taking place in ATR.

The reaction conditions ($H_2O/C$ and $O_2/C$ feed ratios, temperature and pressure) were optimised with thermodynamic calculations and experimentally to reduce the amount of unwanted side products and the formation of coke (Papers I and II). The formation of coke and light hydrocarbons can be reduced by adding excess steam ($H_2O/C > 1$ mol/mol) and oxygen to the feed (ATR) [34]. Unfortunately, the addition of oxygen decreases the *Ref/Ox* molar ratio (Eq. 19) of the product because oxidation reactions become more important and larger amounts of $CO_2$ and $H_2O$ are produced. The $O_2/C$ molar ratio was optimised with the equations below (Eqs. 20–21) with the aim of achieving a thermoneutral overall reaction. The calculations were based on the stoichiometry of the SR (Eq. 2) and POX (Eq. 3) reactions by assuming that all oxygen was consumed in the POX reaction and the fuel was fully (100%) converted in the SR or POX reactions. With a $H_2O/C$ molar ratio of 3 mol/mol, the optimal $O_2/C$ molar ratio for ATR of *n*-heptane is 0.34 mol/mol. (Paper II)

$$X_{SR} + X_{POX} = 100\% \tag{20}$$

$$X_{SR}\Delta H^{\circ}{}_{SR} = -X_{POX}\Delta H^{\circ}{}_{POX} \tag{21}$$

The contribution of side reactions, such as the WGS reaction (Eq. 6) and methanation (Eq. 22), to the product distribution and the thermoneutrality of ATR reactions was examined (Paper II). According to thermodynamic calculations, owing to the excess of water ($H_2O/C$ = 3 mol/mol), the equilibrium WGS conversion of carbon monoxide at 700 °C would be about 60%. The methanation equilibrium reaction (Eq. 22), on the other hand, does not affect the ATR product beyond 616 °C, where the Gibbs free energy for methanation is $\Delta G^{\circ} > 0$ kJ/mol (Paper II).

$$3H_2 + CO \Leftrightarrow CH_4 + H_2O \qquad \Delta H^{\circ}{}_{298} = -206.2\ kJ/mol \tag{22}$$

The thermodynamics for carbon formation were calculated. The Boudouard reaction (Eq. 8) is thermodynamically favoured at $T < 700$ °C and the disproportionation of $CH_4$ (Eq. 10) at $T > 540$ °C (Figure 8). Thus, at optimal reforming temperature (700 °C) carbon formation via both reactions is possible, and the role of the catalyst becomes crucial. Both reactions are reversible [17], however, and they can be controlled with the reaction conditions. The dissociation reactions of hydrocarbons (Eq. 7) are catalysed, among others, by nickel, and the whisker carbon growth under nickel particles [24,34] could lead to breakdown of the catalyst. The hydrocarbon ($C_xH_y$) dissociation reactions (Eq. 7) are irreversible for x > 1, moreover. [18,24]

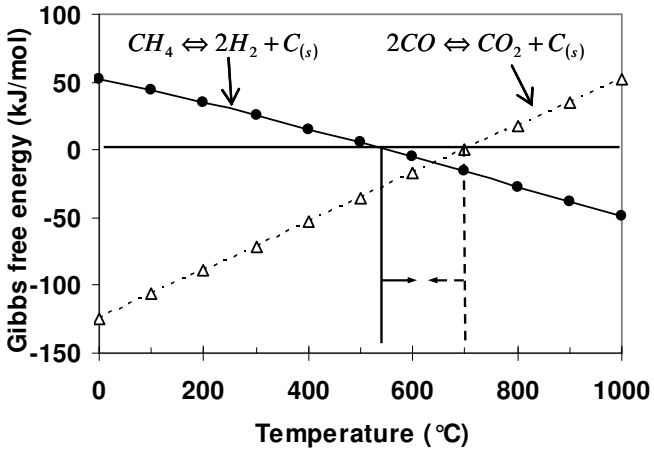


Figure 8. Gibbs free energy $\Delta G°$ (kJ/mol) for $CH_4$ (●) and CO (△) dissociation reactions as a function of temperature.

## 3.2 Comparison of steam reforming and autothermal reforming

SR ($H_2O/C$ = 3 mol/mol) and ATR ($H_2O/C$ = 2.92–3.37 mol/mol, $O_2/C$ = 0.25–0.34 mol/mol) of liquid hydrocarbon fuels were compared on the conventional 15 wt% $NiO/Al_2O_3$ catalyst with *n*-heptane as the model compound (Paper I). In both processes, the main products were $H_2$, CO, $CO_2$ and $CH_4$, and with an increase in *n*-heptane conversion (obtained by varying *GHSV* or *T*) the selectivity for $H_2$ increased and that for $CH_4$ decreased (Figure 9). This may suggest that *n*-heptane is first converted to $CH_4$, which then reacts further to synthesis gas. With a low reforming rate, moreover, coke formation and thermal cracking were detected.

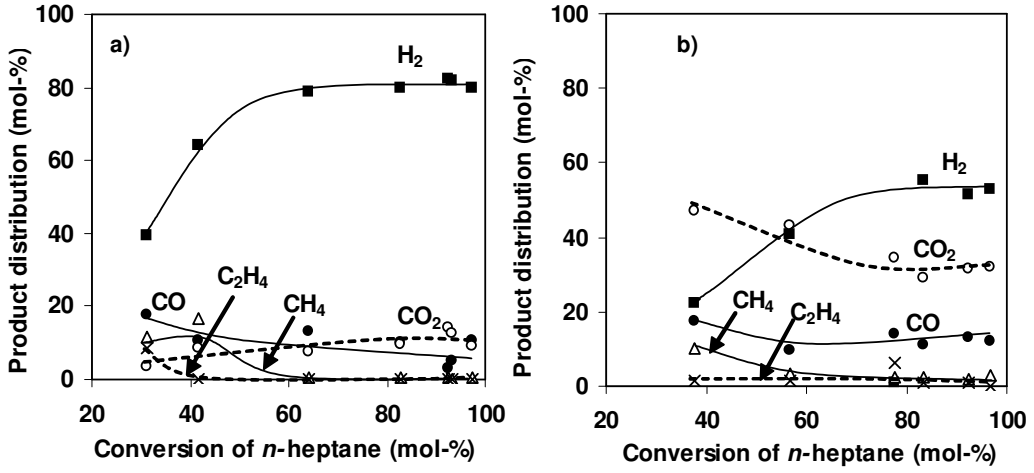


Figure 9. The product distribution ($H_2$ (■), CO (●), $CO_2$ (○), $CH_4$ (△) and $C_2H_4$ (×)) in a) SR ($H_2O/C$ = 3 mol/mol) and b) ATR ($H_2O/C$ = 2.29–3.37 mol/mol, $O_2/C$ = 0.25–0.34 mol/mol) as a function of *n*-heptane conversion on the 15 wt% $NiO/Al_2O_3$ catalyst. $GHSV = 1.6 \cdot 10^5$–$4.7 \cdot 10^5$ 1/h, $T$ = 500–725 °C. (Paper I)

As expected, the conversion of *n*-heptane was higher in ATR than in SR. However, the maximum selectivity for $H_2$ was higher for SR (80%) than for ATR (53%), while the formation of $CO_2$ was lower (Figure 9). This also corresponds to the thermodynamics. In SR, the pressure drop over the catalyst bed increased due to coke formation, as was verified by the semi-quantitative carbon determination of the tested catalysts. In ATR the coke accumulation and the catalyst deactivation were reduced by the presence of oxygen. Some coke deposition was nevertheless observed and the 15 wt% $NiO/Al_2O_3$ catalyst deactivated with time in ATR as in SR.

### 3.3 Comparison of hydrocarbon model compounds

ATR of hydrocarbon model compounds and their mixtures was studied in non-catalytic experiments and on the 15 wt% $NiO/Al_2O_3$ catalyst to determine the characteristics and differences in the reactivity of aliphatic and aromatic hydrocarbons and the influence of the fuel molecular structure on the product distribution.

### 3.3.1 Non-catalytic experiments

Thermal stability of the model compounds was examined under optimised ATR conditions ($H_2O/C$ = 3 mol/mol, $O_2/C$ = 0.34 mol/mol) between 400 and 900 °C in the absence of a catalyst. The SR conditions ($H_2O/C$ = 3 mol/mol, $O_2/C$ = 0 mol/mol) were studied for comparative purposes.

With single hydrocarbons and their mixtures, the thermal cracking was negligible at low temperatures (400–500 ºC). The conversions of the aliphatic hydrocarbons increased with temperature, *n*-dodecane being the most reactive of the hydrocarbons studied (Figure 10). The aromatic hydrocarbon, toluene, started to react thermally only at 800 °C and was the only hydrocarbon that did not react completely at the studied temperatures (Paper II).

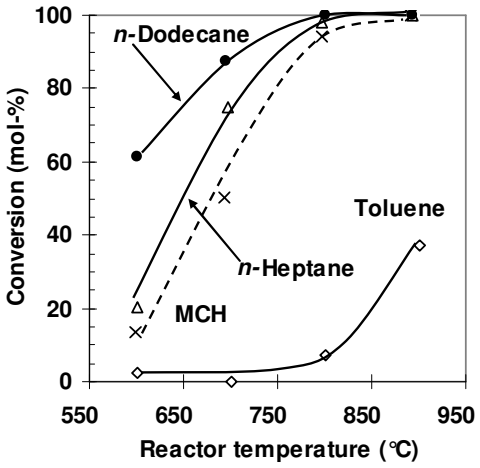


Figure 10. Conversions of *n*-dodecane (●), *n*-heptane (△), methylcyclohexane (MCH) (×) and toluene (◇) in thermal cracking experiments with single hydrocarbons. $H_2O/C$ = 3 mol/mol, $O_2/C$ = 0.34 mol/mol, $V_{Reactants}$ = 300 $cm^3/min_{NTP}$. (Paper II)

With hydrocarbon mixture MHT, the conversions of *n*-heptane, methylcyclohexane and oxygen increased with temperature, and complete decomposition of *n*-heptane and methylcyclohexane was reached at the inlet temperature of 750 ºC (Paper IV, Figure 3), which is in agreement with thermal cracking reactions of the individual hydrocarbons (Figure 10). Toluene, on the other hand, was formed at temperatures below 700 ºC

(Paper IV, Figure 3), indicating *n*-heptane dehydrocyclisation or methylcyclohexane dehydrogenation to toluene and $H_2$. At temperatures higher than 700 ºC, more toluene was converted than was produced, and at 900 ºC decomposition was almost complete. The negative value obtained for the water conversion at 700–900 °C and the sharp increase in oxygen consumption indicated the formation of water by OX (Eq. 5). (Paper IV)

The main products of thermal cracking were $H_2$, CO, $CO_2$, ethene, methane and propane. Hydrogen was formed in greatest amount in reactions of *n*-dodecane and in least amount in reactions of toluene. Most ethene was formed in reactions of *n*-heptane and hardly any in reactions of toluene, which is in agreement with the results of Flytzani-Stephanopoulos and Voecks [58]. The formation of ethene accelerated with temperature up to 900 °C, when it finally declined. Carbon oxides were not detected in SR conditions but only in ATR conditions. Hence, light hydrocarbons and $H_2$ must have been formed via thermal cracking of the feed, whereas carbon oxides must have been formed mainly through oxidation reactions. In the absence of the catalyst the conversion of oxygen reached 100% only at 900 °C.

To conclude, thermal cracking reactions may be present in the reforming of liquid hydrocarbons, aliphatic hydrocarbons being more reactive than aromatic hydrocarbons [58]. The reactivity increased with the length of the hydrocarbon chain, moreover. High reforming activity of the catalyst is required to suppress the presence of thermal reactions of aliphatic hydrocarbons. In other words, the presence of thermal cracking products (i.e., light hydrocarbons) indicates low catalyst activity.

### 3.3.2 Experiments with the conventional 15 wt% $NiO/Al_2O_3$ catalyst

ATR conversions of *n*-dodecane, *n*-heptane, methylcyclohexane and toluene were compared on the 15 wt% $NiO/Al_2O_3$ catalyst. The conversion of *n*-dodecane was almost 100% over the whole temperature range investigated (700–900 °C), whereas the conversions of *n*-heptane, methylcyclohexane and toluene improved with temperature (Paper II; Figure 2). Thus, *n*-dodecane was the most reactive hydrocarbon and toluene the most stable, which is in agreement with their conversions in thermal experiments (Figure 10) and with thermodynamic calculations.

The main products of ATR on the nickel catalyst were $H_2$, CO and $CO_2$ (Table 4). The selectivity for hydrogen increased with temperature and the hydrocarbon conversions (Papers I and II). Side products, such as ethene, methane and small amounts of other light hydrocarbons, were formed in ATR of the aliphatic hydrocarbons. Indeed, in addition to accelerating with temperature, thermal cracking always took place when the ATR conversion of the aliphatic hydrocarbons was incomplete. Thermal cracking products were not detected in ATR of toluene, even though the reforming conversion was incomplete.

Table 4. Conversions and main products in ATR of single hydrocarbons on the 15 wt% $NiO/Al_2O_3$ catalyst at the inlet temperature of 700 °C. $H_2O/C$ = 3 mol/mol, $O_2/C$ = 0.34 mol/mol, $GHSV = 3.6 \cdot 10^5$ 1/h. (Paper II)

| | $T_{cat.\ bed}$ (°C) | Conversion (mol-%) | Main product distribution (mol-%) | | | | |
|---|---|---|---|---|---|---|---|
| | | | $H_2$ | CO | $CO_2$ | $CH_4$ | $C_2H_4$ |
| Toluene | 720 | 71 | 36 | 26 | 36 | 0.2 | 0.0 |
| Methylcyclohexane | 730 | 83 | 49 | 28 | 22 | 0.1 | 0.2 |
| *n*- Heptane | 720 | 85 | 53 | 20 | 19 | 2.0 | 2.6 |
| *n*- Dodecane | 720 | 100 | 60 | 18 | 20 | 0.1 | 0.0 |

The greater stability of aromatic than of aliphatic hydrocarbons means that higher reforming temperatures are required for fuels containing aromatic compounds, and the possibility for thermal reactions is thereby increased. In ATR of toluene, moreover, coke formation was stronger than with the aliphatic hydrocarbons, and the nickel catalyst deactivated with time. Because of the tendency for coke formation, the presence of aromatic or polyaromatic hydrocarbons (PAHs) makes the ATR of commercial fuels highly challenging. Stable catalysts that tolerate coke and, unlike nickel catalysts [59], do not promote coke formation are required.

# 4 Noble metal catalysts

Strong coke accumulation was observed in SR and ATR of hydrocarbon model compounds on the conventional Ni-based catalyst. The coke formation caused catalyst deactivation and promoted thermal cracking reactions. The catalyst particles also exhibited some crumbling during the ATR due to carbon formation under the active nickel particles [34], and this increased the pressure drop over the catalyst bed. Indeed, owing to the tendency for formation of carbon nanofibre (whisker carbon), the conventional Ni-based catalysts are highly sensitive to coke formation [24,34,59]. Furthermore, nickel does not tolerate the sulfur [17] present in commercial fuels. Noble metal catalysts, in contrast, are highly tolerant of sulfur [7,31] and resistant to coke formation [7,24,31].

A series of $ZrO_2$-supported mono- (Rh, Pd, Pt) and bimetallic (RhPt) catalysts were prepared, with a targeted total metal loading of 0.5 wt%. The catalysts were characterised (Papers III and IV) and investigated in ATR of simulated fuels (i.e., DT and MHT mixtures) in optimised reaction conditions ($H_2O/C$ = 2.3–3 mol/mol, $O_2/C$ = 0.34 mol/mol). The catalytic performance of $ZrO_2$-supported noble metal catalysts was compared with that of the conventional 15 wt% $NiO/Al_2O_3$ catalyst and of the $ZrO_2$ support. (Papers II-IV)

## 4.1 Monometallic Rh, Pd and Pt catalysts

The monometallic rhodium catalyst was superior to the palladium and platinum catalysts in both reforming activity and selectivity. On $Rh/ZrO_2$, high hydrocarbon and water conversions were obtained at the inlet temperature of 700 °C (Table 5), correlating with the activity of 15 wt% $NiO/Al_2O_3$.

Table 5. Conversions and main products in ATR of DT mixture on Rh(700), Pd(700), Pt(700) and $ZrO_2$ at the inlet temperature of 700 °C. $H_2O/C$ = 2.3 mol/mol, $O_2/C$ = 0.34 mol/mol, $GHSV = 3.0 \cdot 10^5$ 1/h. (Paper III)

| | $T_{cat.\ bed}$ | Conversion (mol-%) | | Main product distribution (mol-%) | | | | | $CO/CO_2$ |
|---|---|---|---|---|---|---|---|---|---|
| | | DT | $H_2O$ | $H_2$ | CO | $CO_2$ | $CH_4$ | $C_2H_4$ | (mol/mol) |
| Rh(700)* | 695 | 100 | 24 | 63 | 16 | 21 | 0.5 | 0.0 | 0.76 |
| Pd(700)* | 730 | 80 | -3 | 54 | 30 | 12 | 1.1 | 1.8 | 2.5 |
| Pt(700)* | 760 | 70 | -11 | 22 | 44 | 15 | 2.7 | 8.4 | 2.9 |
| $ZrO_2$ | 700 | 70 | -4 | 16 | 39 | 12 | 4.3 | 14 | 3.3 |

* *Catalyst calcination temperature (700 °C) indicated in parentheses.*

The main products were $H_2$, CO and $CO_2$, and no undesired side products (ethene) were detected. Thus, thermal cracking was suppressed by the high ATR activity of rhodium (Paper II). However, fast consecutive conversion of the products of thermal cracking can not be excluded. The high conversions of water indicated strong SR, which was further verified by the low temperature of the catalyst bed. (Papers II and III)

On $Pd/ZrO_2$ and $Pt/ZrO_2$, the hydrocarbon conversions at 700 °C were incomplete and more water was produced (OX, Eq. 5) than was consumed resulting in negative values of the conversion (Table 5). Moreover, thermal cracking products were detected in the product, which indicated low ATR activity. The activity of palladium and platinum improved with temperature, however, as was noticed in the improved hydrocarbon and water conversions and in the decrease of thermal cracking products (Paper III). The competition between ATR reactions and thermal cracking was especially evident on $Pt/ZrO_2$. That is, the formation of ethene and other alkenes increased with temperature up to 800 °C, where it finally declined (Paper III, Figure 3b). At 900 °C, the ATR activity of platinum was sufficient to suppress thermal cracking.

The activities of the catalysts in SR and oxidation (OX and POX) correlated with the temperature profiles over the catalyst bed. Exothermic reactions predominated on $Pt/ZrO_2$ and $Pd/ZrO_2$, whereas an overall endothermic reaction was seen on $Rh/ZrO_2$ (Paper III, Figure 5). Furthermore, the conversion of oxygen was incomplete in the thermal experiments and on $ZrO_2$, but 100% in the presence of noble metals. The noble metal must, therefore, also play a critical role in the oxidation reactions (OX and POX), and both the SR and the oxidation are taking place on the active sites of the catalyst. In experiments on $ZrO_2$, thermal cracking was present over the whole temperature range and water was continually produced in greater amounts than it was consumed, indicating low reforming activity.

On $Rh/ZrO_2$ and $Pd/ZrO_2$, a decrease in the hydrocarbon and water conversions and degradation of the product distribution occurred with time. Also the increasing formation of thermal cracking products, mainly ethene, reflected a change in the catalyst structure and poor stability of the catalyst. On $Pt/ZrO_2$, where thermal cracking products were formed in highest amounts and the average rate of carbon deposition at 700 °C was higher (0.55–0.88 $mgC/g_{cat}/h$) than on $Rh/ZrO_2$ (0.37–0.54 $mgC/g_{cat}/h$) (Paper IV), the catalyst performance did not deteriorate with time. Similar results – deactivation of rhodium catalyst and stability of platinum catalyst – have been reported for SR of biomass-derived pyrolysis oil [60].

The high $CO/CO_2$ molar ratio obtained on $Pt/ZrO_2$ (2.9 mol/mol, Table 5) reveals the presence of the reverse-Boudouard reaction (Eq. 8), favoured by the thermodynamics. This observation is in good agreement with the results of $CO_2$ pulsing experiments performed by Bitter et al. [61] on coked $Pt/ZrO_2$. Since the deposited coke is also removed from the catalyst surface, a steady state for the coke amount is conceivable. The carbon deposition rate corresponds to that reported by Souza and Schmal for $Pt/ZrO_2$ catalysts tested in the DR of methane (0.8–0.9 mg $coke/g_{cat}/h$) [62]. The high $CO/CO_2$ molar ratio obtained on $ZrO_2$ (3.3 mol/mol, Table 5) is explained by the ability of the $ZrO_2$ to release oxygen, which promotes the formation of CO [61].

Although coke formation was detected on all the $ZrO_2$-supported noble metal catalysts, these catalysts were considerably more resistant to coke formation than was the nickel catalyst. Furthermore, less than 0.01 mol% of the fed carbon (2.9 mmol C/min) was

accumulated. Nonetheless, the active $Rh/ZrO_2$ catalyst exhibited extremely low thermal stability, as Rh depletion [40] from the catalyst was dramatic in the oxidising environment of the regeneration step performed with air. (Paper II)

## 4.2 Bimetallic RhPt catalysts

Bimetallic RhPt catalysts were prepared with the aim of combining the activity of rhodium in SR with the stability of platinum. Platinum also contains active sites for exothermic POX, and RhPt catalysts should thus be ideal for thermoneutral ATR of commercial fuels. The $ZrO_2$-supported RhPt catalysts were compared with monometallic rhodium and platinum catalysts in ATR of simulated fuels (400–900 °C). The effects of *Rh/Pt* molar ratio (0.5, 1 and 2 mol/mol) and calcination temperature (700 °C and 900 °C) on the catalyst performance were investigated. (Paper IV)

High catalytic activity was observed for all the bimetallic catalysts. Thus, just a small amount of rhodium in the bimetallic catalyst was sufficient to improve the catalyst performance over that of the monometallic $Pt/ZrO_2$. Still, monometallic $Rh/ZrO_2$ was most active for SR. The Rh-containing catalysts also supported high activity for the WGS reaction (Eq. 6), which affected the product yields within the whole temperature range, as can be seen for 2RhPt(900) in Figure 11.

The catalyst selectivity for reforming was examined as the *Ref/Ox* molar ratio (Eq. 19) of the product where the effect of the WGS reaction is neglected (Paper III). The WGS reaction was strongly present with all Rh-containing catalysts and, because of the WGS equilibrium, the water conversion levelled off at 700 °C (Paper IV, Figure 4b). On $Pt/ZrO_2$, on the other hand, the WGS equilibrium did not have a noticable effect on the product distribution. The selectivity for reforming was highest on the bimetallic 1RhPt and 2RhPt catalysts. The reforming selectivity of Pt was lower than that of the bimetallic catalysts because of the greater activity for oxidation reactions and the presence of thermal cracking. (Paper IV)

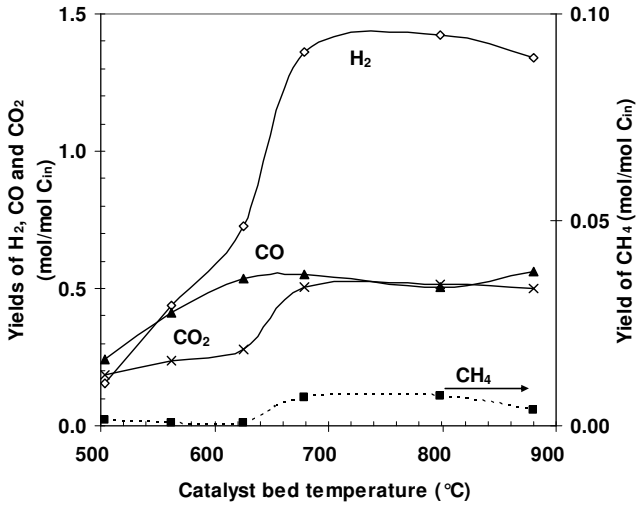


Figure 11. Yields of $H_2$ (◇), CO (▲), $CO_2$ (×) and $CH_4$ (■) in ATR of MHT mixture on 2RhPt(900)/$ZrO_2$. $H_2O/C$ = 3 mol/mol, $O_2/C$ = 0.34 mol/mol, $GHSV = 3.1 \cdot 10^5$ 1/h. (Paper IV)

In short-term stability tests (700 °C for 5–6 hours) performed with bimetallic RhPt catalysts, neither a decrease in the conversions nor the formation of thermal cracking products was observed. Thus, only a small amount of platinum in the bimetallic catalysts is sufficient to improve the stability over that of the monometallic Rh/$ZrO_2$ catalyst. The stability of the bimetallic RhPt catalysts improved with an increase in the *Rh/Pt* ratio (Paper IV), which was also reflected in the lower rates of carbon formation.

Higher calcination temperature (900 °C) had a slightly negative effect on the physical properties (e.g., BET surface area and total pore volume) but stabilised the surface structure of both the mono- and bimetallic RhPt catalysts (Paper IV). Moreover, at elevated calcination temperature carbon deposition increased with higher Pt loading of the catalyst and decreased with higher Rh loading. The results for carbon deposition agreed with those for catalyst activity, selectivity and stability, as carbon deposition was lowest on the bimetallic catalysts (especially 2RhPt/$ZrO_2$) where the hydrogen formation was stable and the *Ref/Ox* ratio highest.

To conclude, in terms of selectivity (*Ref/Ox*, Eq. 19) and stability, bimetallic RhPt catalysts were superior to the monometallic rhodium and platinum catalysts, and the catalyst performance could be controlled with the *Rh/Pt* ratio.

# 5 ATR of simulated and commercial fuels

The bimetallic RhPt catalysts demonstrated high catalytic performance – activity, selectivity and stability – in the ATR of simulated fuels. $H_2$-rich fuel gas was successfully produced under sulfur-free conditions. Next, the sulfur tolerance of $ZrO_2$-supported RhPt catalysts was investigated, and the suitability of sulfur-containing commercial fuels (low-sulfur diesel) as hydrogen source and as primary fuel for high temperature fuel cell applications was evaluated.

## 5.1 RhPt catalysts in ATR of low-sulfur diesel

Rh(900), Pt(900) and 2RhPt(900) catalysts were examined in ATR of low-sulfur diesel. Table 6 presents the conversions and dry product distribution obtained on these catalysts at 700 °C. The conversions were highest on the bimetallic catalyst. The low conversions obtained on Pt, with the formation of thermal cracking products (designated as “others” in Table 6), indicated low reforming activity. Thus, the differences between these catalysts were similar to the differences described for ATR of the simulated fuels under sulfur-free conditions (Section 4.2, and Papers III and IV).

At 700 °C, where the conversion of fuel was incomplete, deactivation occurred with time, and the product distribution was degraded. The oxygen conversion decreased from 97% to 89% on Pt, but not on the Rh-containing catalysts, indicating that the sites of the Pt active for oxidation became blocked, or else sintering of Pt occurred [44,63]. On all

catalysts the conversions and the product distribution improved with temperature, and at 900 °C the conversion of diesel was almost complete (99–100%). (Paper V)

Table 6. Conversions and dry product distribution in ATR of low-sulfur diesel on $ZrO_2$-supported mono- and bimetallic RhPt catalysts after 1 hour on stream. $T$ = 700 °C, $H_2O/C$ = 3 mol/mol, $O_2/C$ = 0.34 mol/mol, $GHSV = 3.1 \cdot 10^5$ 1/h. (Paper V)

| | **Conversion (mol-%)** | | | **Product distribution (mol-%)** | | | | |
|---|---|---|---|---|---|---|---|---|
| | **Diesel** | **$H_2O$** | **$O_2$** | **$H_2$** | **CO** | **$CO_2$** | **$CH_4$** | **Others** |
| Rh(900)* | 72 | 8.3 | 99 | 46 | 29 | 6.9 | 0.5 | 17 |
| 2RhPt(900)* | 77 | 19 | 99 | 55 | 26 | 11 | 0.5 | 7.0 |
| Pt(900)* | 25 | -5.8 | 97 | 7.7 | 17 | 34 | 2.8 | 39 |

* *Catalyst calcination temperature (900 °C) indicated in parentheses.*

The thermal stability of the 2RhPt(900) catalyst was studied at 900 °C (5 hours). The selectivity for $CO_x$ and the *Ref/Ox* molar ratio (Eq. 19) remained constant throughout the experiment. The product distribution and the conversion of water, on the other hand, changed along the run, and the molar ratios of $CO/CO_2$ and $(H_2O+CO)/(H_2+CO_2)$ (reverse WGS, Eq. 6) increased linearly with time. Since the selectivity for $CO_x$ remained constant, the Boudouard reaction (Eq. 8) was not causing the shift in the $CO/CO_2$ ratio. The reverse WGS reaction, where the moles of formed CO and consumed $CO_2$ are equal, must have been taking place instead. This change in the catalyst selectivity indicated a change in the catalyst structure, which in the long-run experiments could affect the catalyst stability. However, in the short term runs (5 h), no drop in the conversion of the diesel was observed at high temperatures (900 °C).

The reaction temperature of ATR of low-sulfur fuels turned out to be crucial with all the mono- and bimetallic RhPt catalysts, as irreversible deactivation of the Rh-containing catalyst was observed during experiments at temperatures below 700 °C. Although the conversions and product distribution improved with temperature, initial levels were not recovered. (Paper V)

## 5.2 $H_2S$ and 4,6-DMDBT as sulfur model compounds

ATR of simulated fuels (i.e., DT and MHT mixtures) was investigated on 2RhPt(900) with $H_2S$ and 4,6-DMDBT added as sulfur model compounds (10 ppm S in fuel). The results were compared with those for ATR performed in sulfur-free conditions and for ATR of commercial low-sulfur diesel (Figure 12).

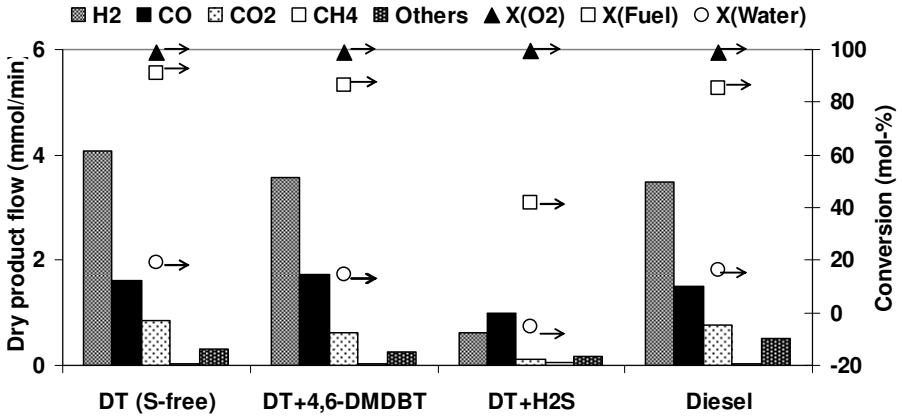


Figure 12. The effect of sulfur compounds on the conversions ($O_2$ (▲), fuel (□) and $H_2O$ (○)) and dry product flows (mmol/min) in ATR of simulated (DT) and commercial, low-sulfur fuels (diesel) on 2RhPt(900)/$ZrO_2$ at the inlet temperature of 700 °C. $H_2O/C$ = 3 mol/mol, $O_2/C$ = 0.34 mol/mol, $GHSV = 3.1 \cdot 10^5$ 1/h, S 10 ppm. (Paper V)

The product distribution and the conversions obtained in sulfur-free ATR of simulated fuel corresponded well with the results for ATR of commercial diesel, and the addition of 4,6-DMDBT improved the correspondence (Figure 12). In the presence of this heterocyclic sulfur compound, the conversion of the fuel decreased slightly with time, indicating some deactivation of 2RhPt(900). The effect of 4,6-DMDBT on the catalyst performance was not marked, however, and $H_2S$ was at no time detected in the product flow (400–900 °C). It bears notice that 4,6-DMDBT is the most stable heterocyclic sulfur compound, and thus, may not represent other heterocyclic sulfur compounds possibly present in commercial fuels.

With $H_2S$ as the sulfur model compound, immediate deactivation of the 2RhPt(900) catalyst took place and the fuel conversion was incomplete over the whole temperature range (400–900 °C). The catalyst activity for reforming was almost totally lost at lower temperatures, as conversions of fuel and water in the presence of $H_2S$ were similar to those obtained on $ZrO_2$ and in thermal cracking reactions performed in sulfur-free conditions (Paper IV). In other words, mostly $H_2$ oxidation to $H_2O$ took place resulting in negative conversion of water. The catalyst performance remained stable in the presence of $H_2S$, however, confirming that a steady state prevailed between the sulfur compounds present in the gas phase and adsorbed on the catalyst surface. Furthermore, the presence of $H_2S$ did not hinder the oxidation reactions (POX, OX) taking place, as the conversion of oxygen (100%) was not affected at any temperature studied (400–900 °C). Only the activity for reforming was degraded.

The low reforming activity of the 2RhPt(900) catalyst in the presence of $H_2S$ could be compensated with elevated temperature. $H_2S$ accumulated strongly at temperatures below 700 °C but it desorbed at 900 °C, and the catalyst was reactivated; simultaneously the amount of thermal cracking products decreased (Paper V). In fact, the same reforming activity was obtained at 900 °C in the presence of $H_2S$ as was obtained at 700 °C in sulfur-free conditions and in the presence of 4,6-DMDBT. The influence of $H_2S$ was mostly reversible, as the catalyst activity at 700 °C recovered rapidly when the $H_2S$ flow was turned off (Paper V, Figure 7). Although the reactivation of the catalyst continued with time, the initial conversion and product distribution were not regained, indicating some irreversible adsorption of $H_2S$ [64].

Figure 13 compares the effect of different sulfur compounds on the selectivity of the 2RhPt(900) catalyst for reforming (*Ref/Ox*, Eq. 19). The heterocyclic sulfur compounds (4,6-DMDBT in DT and those in commercial diesel) scarcely affected the selectivity, and the *Ref/Ox* ratio predicted by the thermodynamics was reached at 700 °C. The presence of $H_2S$, in turn, degraded both the reforming activity and selectivity, and the oxidation reactions predominated ($X_{O2}$ = 100%) over the entire temperature range studied. Furthermore, the results obtained with commercial diesel on the deactivated

2RhPt(900) catalyst were better than the results obtained in the presence of $H_2S$ (Figure 13).

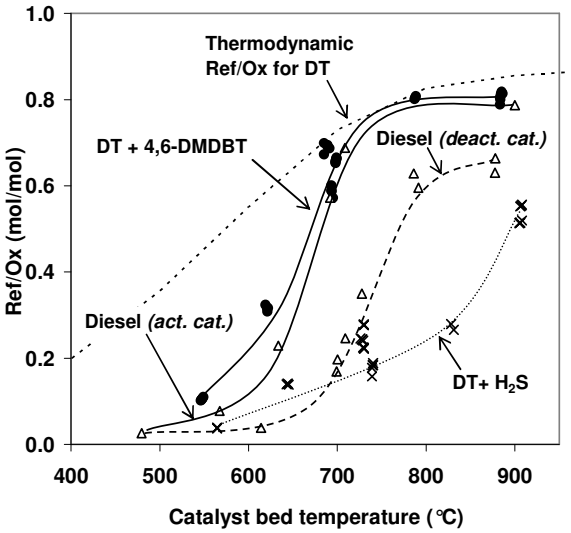


Figure 13. The *Ref/Ox* molar ratio (($H_2$+CO)/($H_2O$+$CO_2$)) of the ATR product of commercial diesel (△) and simulated fuels (DT) in the presence of 4,6-DMDBT (●) and $H_2S$ (×) on $ZrO_2$-supported 2RhPt(900). For diesel: active catalyst (solid line), deactivated catalyst (dash line). $H_2O/C$ = 3 mol/mol, $O_2/C$ = 0.34 mol/mol, *GHSV* = $3.1 \cdot 10^5$ 1/h, S 10 ppm. (Paper V)

As is evident from Figure 12, both sulfur compounds had a clear effect not only on the conversions of the fuel and water but also on the product distribution. Both $H_2S$ and 4,6-DMDBT decreased the amount of $CO_2$ produced (Figure 12), thereby increasing the CO/$CO_2$ ratio of the product, even though the conversion of oxygen was not affected. In the presence of $H_2S$, moreover, the CO/$CO_2$ ratio also increased dramatically with temperature, reaching a maximum (13.7 mol/mol) at 800 °C; with 4,6-DMDBT the ratio reached a considerably lower maximum (6.0 mol/mol) at 700 °C. Hence, sulfur had a clear effect on the side reactions – WGS (Eq. 6) and Boudouard (Eq. 8) reactions. (Paper V)

## 5.3 Sulfur and carbon deposition

The sulfur and carbon contents of the mono- and bimetallic catalysts (Rh(900), Pt(900), 2RhPt(900)) were determined before and after ATR of the simulated and commercial fuels (Table 7).

Table 7. Sulfur and carbon deposition on the $ZrO_2$-supported Rh(900), Pt(900) and 2RhPt(900) catalysts tested in ATR of commercial (low-sulfur diesel) and simulated (MHT) fuels. $H_2O/C$ = 3 mol/mol, $O_2/C$ = 0.34 mol/mol, $GHSV = 3.1 \cdot 10^5$ 1/h, S 10 ppm. (Paper V)

| Fuel | Catalyst | Sulfur ($\mu g/g_{cat}/h$) | Carbon ($mg/g_{cat}/h$) | $CO/CO_2$ (average, mol/mol) |
|---|---|---|---|---|
| Diesel[a] | 2RhPt(900) | 5.6 | 3.7 | 2.2 |
| Diesel[a] | Pt(900) | 12 | 4.9 | 0.5 |
| Diesel[a] | Rh(900) | 21 | 2.0 | 4.9 |
| MHT[b] | 2RhPt(900) | 0.0 | 0.95 | 2.1 |
| MHT+4,6-DMDBT[b] | 2RhPt(900) | 2.3 | 1.2 | 2.6 |
| MHT+$H_2S$[b] | 2RhPt(900) | 30 | 0.73 | 3.4 |

[a] *ATR of diesel performed at 700 °C (5 hours).*

[b] *ATR of simulated fuels studied at 400-900 °C.*

In ATR of commercial diesel, the amount of sulfur was highest on Rh(900) and lowest on 2RhPt(900) (Table 7). Moreover, the amount of sulfur on the 2RhPt(900) catalyst was low in the presence of heterocyclic sulfur compounds (i.e., 4,6-DMDBT and low-sulfur diesel) and clearly higher in the presence of $H_2S$. Still, just 0.08 wt% of the total sulfur feed flow (35.7 $mgS/g_{cat}/h$) was deposited on the catalyst in the $H_2S$ experiment (5 hours), and the molar ratio of sulfur to noble metal was only 0.13.

According to visual estimation, the amount of coke deposited on the 2RhPt(900) catalyst particles was greatest after ATR of low-sulfur diesel; virtually no coke was detected after the experiment with $H_2S$. This result was verified by carbon determination (Table 7). The complex nature of commercial fuels, which contain several aromatic compounds (coke precursors), explains the stronger deactivation of the RhPt catalyst in ATR of the low-sulfur diesel than in ATR of the simulated fuels in both the presence and absence of sulfur. However, the coke that was formed was partly removed from the catalyst during ATR, and the oxygen feed assisted in the coke

removal from the catalyst surface [15], especially at high temperatures (900 °C). (Paper V)

In ATR of low-sulfur diesel, coke deposition on the Rh(900), Pt(900) and 2RhPt(900) catalysts was visibly different and this correlated with the measured amounts of carbon (Table 7). The average carbon deposition in ATR of low-sulfur diesel was directly proportional to the Pt loading of the catalyst and increased in the order Rh < RhPt < Pt. Moreover, the $CO/CO_2$ ratio decreased linearly with an increase in the Pt loading, in contrast to what occurred under sulfur-free conditions, where the $CO/CO_2$ molar ratio of the product was highest on $Pt/ZrO_2$. Indeed, in sulfur-free conditions, the reverse-Boudouard reaction (Eq. 8) was strongly present on $Pt/ZrO_2$ (Paper IV). These differences in carbon deposition, the $CO/CO_2$ molar ratio and the deactivation of the platinum catalyst activity for oxidation indicated the presence of a different type of coke in ATR of low-sulfur diesel than in ATR of the simulated fuels. This coke, moreover, is not removed by the reverse-Boudouard reaction (Eq. 8), as the selectivity for $CO_x$ remained constant.

Considering the catalyst deactivation and the presence of thermal cracking, the amount of carbon that was deposited under the $H_2S$ was extraordinarily low. Thus, the adsorbed sulfur compound derived from $H_2S$ either prevented the deposition of coke by blocking certain active sites of the 2RhPt(900) catalyst [27,65] or promoted coke removal reactions, such as the reverse-Boudouard reaction (Eq. 8) or SR (Eq. 9). Indeed, Suzuki et al. [27] showed that the presence of $H_2S$ prevented CO adsorption on Ru-based catalysts, and similar findings were presented by Strohm et al. [3] for Rh-based catalysts and by Rostrup-Nielsen [65] for Ni-based catalysts. It has also been suggested that the reforming requires a smaller ensemble of active sites than the CO adsorption [3,34,65]. Thus, a certain level of sulfur poisoning minimises the formation of coke but still allows the SR to proceed. Blockage of some of the active sites with $H_2S$ would explain the low conversions and the inhibition of the WGS reaction (Eq. 6), as well as the high content of CO and high $CO/CO_2$ ratio in the product. The active sites for oxidation were not blocked by $H_2S$ since the conversions of oxygen (100%) were not affected. In ATR of

low-sulfur diesel, in contrast, the coke deposition on $Pt/ZrO_2$ essentially reduced the oxidation reactions.

Commercial low-sulfur diesel was successfully simulated with mixtures (DT and MHT) of hydrocarbon model compounds in ATR reactions on $ZrO_2$-supported noble metal catalysts. The addition of a heterocyclic sulfur compound (4,6-DMDBT giving 10 ppm S) improved the similarity. The presence of $H_2S$ (10 ppm S), in contrast, degraded the catalyst performance drastically. That is, the adsorption of $H_2S$ prevented both the reforming and the WGS. Interestingly, it did not interfere with the oxidation reactions, whereas in ATR of low-sulfur diesel, oxidation reactions on $Pt/ZrO_2$ were hindered by strong coke formation. The comparison of mono- and bimetallic RhPt catalysts in ATR of commercial diesel showed, moreover, that the bimetallic 2RhPt catalyst tolerates sulfur better than the corresponding monometallic catalysts. Probably the interaction between Rh and Pt, similarly to the reported interaction between Ni and Rh in the SR of jet fuel [3], prevented binding between the noble metal and sulfur.

# 6 Rh-Pt synergism

In ATR of simulated and commercial fuels, the bimetallic RhPt catalysts were found to be superior to the monometallic rhodium and platinum catalysts in both stability and selectivity. The synergism between Rh and Pt was investigated by several methods.

The BET surface areas and the total pore volumes of the $ZrO_2$-supported catalysts were not affected by the possible interaction between Rh and Pt. Nor were the various adsorption states for CO (DRIFTS) affected when rhodium was combined with platinum in the bimetallic catalyst. However, irreversible $H_2$ uptakes on bimetallic 1RhPt and 2RhPt catalysts were greater than those on the monometallic catalysts, correlating with the better catalytic performance. (Paper IV)

Recently, Kolb et al. [66] claimed that the binary alloys of Rh, Pd, Ir and Pt have been misunderstood for nearly half a century and immiscibility does not exist in the $Rh_xPt_{1-x}$ system below 760 °C [67]. Immiscibility was further disproved by Jacob et al. [68] in thermodynamic measurements. Jacob et al. also described the presence of an alloy-oxide equilibrium in the Rh-Pt-O ternary system measured on an $Y_2O_3$-stabilised $ZrO_2$ solid electrolyte [68,69]. If the $Rh_xPt_{1-x}$ system is miscible, an alloy could be present on the bimetallic catalysts at all *Rh/Pt* ratios. Moreover, the formation of equilibrium between the $Rh_xPt_{1-x}$ alloy and $Rh_2O_3$ is possible in an oxidising environment [69]. It has also been suggested that $Rh_xPt_{1-x}$ alloys result in strong Pt enrichment on the surface with an increase in temperature (maximum at 830 °C) [46,70], and in the presence of oxygen an ordered rhodium oxide overlayer is formed on such Pt-enriched bimetallic

surfaces [71]. Indeed, $Rh_xPt_{1-x}$ alloys have been classified as near-surface alloys (NSAs) owing to the tendency for formation of a subsurface metal layer [72].

Temperature-programmed reduction with hydrogen ($H_2$-TPR) was performed for Rh(700), Pt(700), 2RhPt(700) and 2RhPt(900) catalysts (Paper IV). Two reduction steps (at 95 and 127 °C) were measured on Rh(700), which is in agreement with the TPR measurements performed by Ferrandon and Krause [73], but no reducible species were observed on Pt(700) (Figure 14). Indeed, platinum does not form stable oxides at high temperature [61,69]. Due to low metal loading and analytical limitations, moreover, minor amounts of adsorbed or desorbed hydrogen may not be seen. On the bimetallic 2RhPt catalysts, the presence of platinum and the calcination temperature affected the reducibility of rhodium since only one reduction step was noticed. Moreover, the consumption of $H_2$ was clearly lower with the bimetallic catalysts than with Rh(700) (compare $A_{2RhPt}$ and $A_{Rh}$ in Figure 14). If it is assumed that only Rh compounds reduce and according to the $H_2$ consumption and the rhodium loadings of the catalysts, less than 50% of rhodium atoms on the 2RhPt catalysts were in reducible form, thus indicating the presence of both oxidised and metallic rhodium.

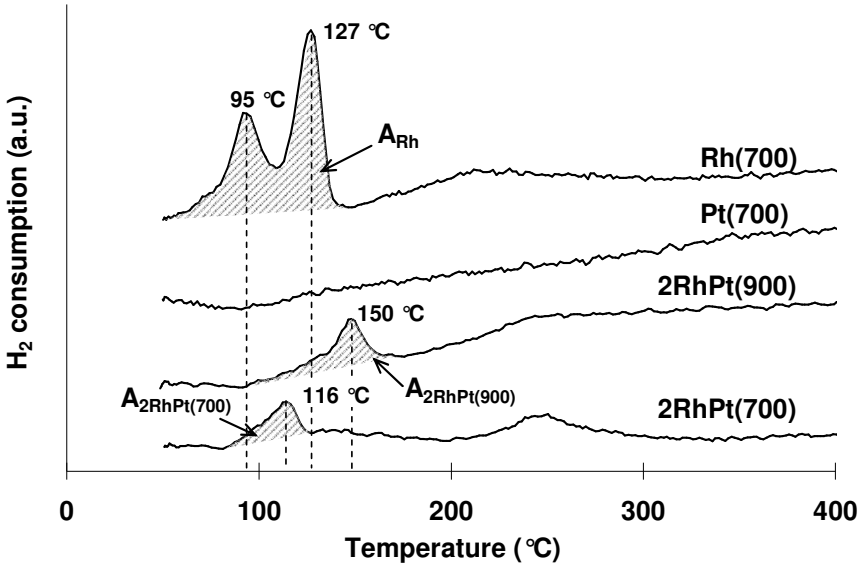


Figure 14. $H_2$ consumption in TPR of Rh(700), Pt(700), 2RhPt(700) and 2RhPt(900). (Paper IV)

SEM and EDX measurements were performed (Paper IV) to examine the surface morphology of the mono- and bimetallic catalysts. No metal clusters were detected on the rhodium catalysts. Thus, either the impregnation procedure was successful and metal particles were well-dispersed, or the rhodium particles were encapsulated within the support [42,43,74]. SEM pictures of the Pt and 2RhPt catalysts showed dispersed metal particles on the surface of the fresh catalyst. On the fresh and used bimetallic catalysts, moreover, the metal particles showed an orthorhombic structure (Figure 15).

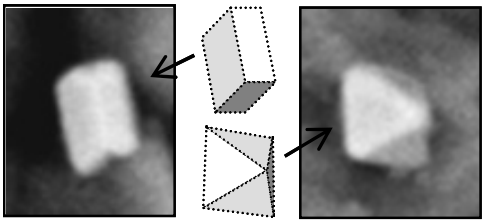

Figure 15. Orthorhombic metal clusters detected on the surface of used 2RhPt(900)/$ZrO_2$.

These orthorhombic crystals differ from the lattice structure proposed for pure rhodium and pure platinum crystals (face-centred cubic (fcc) crystals (Pearson's symbol cF4)) [75] and from the cubo-octahedral shape predicted for $Rh_xPt_{1-x}$ alloy clusters [76]. However, a stable, orthorhombic structure for $Rh_2O_3$ has been confirmed after high temperature (> 500 °C) oxidation treatments [77]. Reducible rhodium species similar to $Rh_2O_3$ are also reported to be the active form of rhodium in three-way catalysts [78], which would explain the high catalytic performance of Rh-containing mono- and bimetallic catalysts also in ATR.

EDX spectra were measured from several metal particles (i.e., orthorhombic crystals) of the 2RhPt(900) catalyst and on the surface of the $ZrO_2$ support. The metal particles of different sizes were found to contain both rhodium and platinum, and the only slight variation in the *Rh/Pt* ratio of the particles allowed the conclusion that the distribution of the two metals was homogeneous. (Paper IV)

According to the TPR, SEM and EDX results and in view of the improved catalyst performance in ATR of simulated and commercial fuels, the presence of the Rh-Pt-O ternary system can be suggested for the bimetallic catalysts, where the metal clusters

consist of a $Rh_xPt_{1-x}$ alloy subsurface and a $Rh_2O_3$ overlayer. Figure 16 presents a scheme for the synergism between rhodium and platinum on the $ZrO_2$ support and the formation of $Rh_xPt_{1-x}$ – $Rh_2O_3$ equilibrium under oxidising conditions.

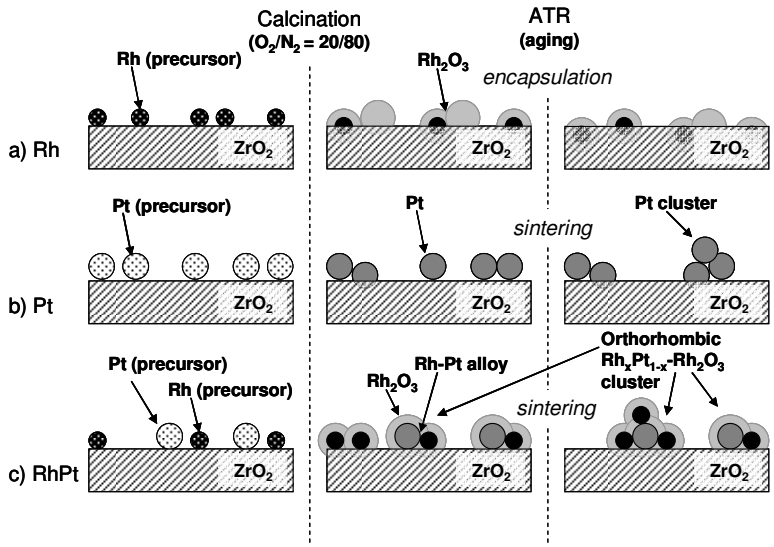


Figure 16. A scheme for the interactions of Pt and Rh on $ZrO_2$-supported a) Rh, b) Pt and c) RhPt catalysts under oxidising conditions of calcination and aging in ATR. (Paper IV)

On the monometallic Rh catalysts, the interaction of rhodium with the support is strong [35] and continues during the aging in ATR (Figure 16a). Moreover, the migration of the support on top of Rh [42,43,73] or the migration of Rh into the support [79] cannot be excluded in the case of $ZrO_2$. Through rhodium encapsulation (Figure 16a), the rhodium of the catalyst is most likely concentrated into subsurface layers of the catalyst, thereby explaining why metal particles were not detected in the SEM measurements of the monometallic Rh catalyst. Subsurface metal layers could still affect the binding of adsorbed species, and thereby the reaction rates and selectivities of the catalytic process [80].

For the reduction of rhodium oxides in strong metal support interaction (SMSI) [35,73] a second reduction step at higher temperature would be needed and this is seen in the TPR curve in Figure 14. SMSI is also observed for $Pt/ZrO_2$ (Figure 16b), and either platinum encapsulation in $ZrO_2$ or even the formation of a Pt-Zr alloy has been

suggested [79]. Since platinum is in metallic state ($Pt^0$), however, the strong interaction with the support is not noticed in the $H_2$-TPR (Figure 14).

The formation of the $Rh_xPt_{1-x}$ alloy on the bimetallic catalysts (Figure 16c) seems to impair SMSI, as has been observed for a bimetallic Ni-Rh catalyst supported on $ZrO_2$ [35]. Hence, the encapsulation of the noble metals (Rh and Pt) is prevented and the $Rh_2O_3$, formed under oxidising conditions, is reduced in a single step. Owing to the $Rh_xPt_{1-x}$ – $Rh_2O_3$ equilibrium, part of the rhodium is present in the reduced state ($Rh^0$), and the consumption of $H_2$ during TPR is less than for the monometallic catalysts (Figure 14).

Suopanki et al. [78] claimed that $Rh_2O_3$ is the active site on Rh-containing catalysts, but the strong interaction of rhodium with $ZrO_2$ and the possible encapsulation of rhodium lead to deactivation of the catalyst with time. According to the present results, however, a slight addition of Pt is sufficient to improve the catalyst performance of the bimetallic catalyst over that of the monometallic catalysts. Through the synergism of rhodium and platinum, a $Rh_xPt_{1-x}$ alloy is formed, which impairs the interaction of the metals with the support [35] (see Figure 16c) and improves the tolerance for sulfur and coke and the selectivity for reforming (Papers IV and V). The amount of active $Rh_2O_3$ can be controlled through the *Rh/Pt* ratio [69,81], temperature and the partial pressure of oxygen, which together determine the $Rh_xPt_{1-x}$ – $Rh_2O_3$ equilibrium in the Rh-Pt-O ternary system [69].

# 7 Conclusions

Steam reforming (SR) of liquid hydrocarbons produces hydrogen with high selectivity. Unfortunately, the reaction enthalpy is high and coke accumulation on the conventional nickel catalyst is significant although steam is fed in excess. Autothermal reforming (ATR) of liquid hydrocarbons is a good alternative to SR. ATR can be carried out in thermoneutral conditions, making possible on-board production of hydrogen in ships for example. Furthermore, in ATR the coke formation can be controlled with the $O_2/C$ feed ratio.

The study was made on the ATR of various hydrocarbon model compounds and their mixtures, and these simulated fuels, with $H_2S$ or 4,6-DMDBT as sulfur compound, were evaluated as models for commercial low-sulfur diesel. Aliphatic hydrocarbons are more reactive than aromatic hydrocarbons, and the reactivity increases with the length of the carbon chain. The higher stability of aromatics means that higher reaction temperatures are required for ATR of commercial fuels containing various aromatic hydrocarbons. With higher temperature, thermal cracking of the fuel accelerates and undesired light hydrocarbons (i.e., ethene and propane) are produced. High catalyst activity is required to suppress these thermal reactions, and at high activities it is essential that the catalyst is resistant to sulfur and coke formation.

$ZrO_2$-supported mono- (Rh, Pd, Pt) and bimetallic (RhPt) noble metal catalysts were studied in ATR of simulated and commercial fuels with the objective of finding stable, active and selective catalysts that also are economically viable. Among the monometallic catalysts, rhodium was most active towards ATR, whereas exothermic

OX and thermal cracking predominated on palladium and platinum catalysts and on $ZrO_2$. The rhodium and palladium catalysts deactivated with time, whereas platinum retained its stability.

The good features of rhodium and platinum were combined in bimetallic RhPt catalysts. Indeed, only a small addition of rhodium improved the activity of the platinum catalyst markedly, and the catalyst performance (i.e., selectivity and stability) could be optimised with the *Rh/Pt* ratio. Strong synergism between rhodium and platinum was observed on the bimetallic catalysts. Catalyst performance was superior as evidenced by the *Ref/Ox* ratio, the rate of hydrogen production and the decreased carbon deposition. The presence of a $Rh_xPt_{1-x}$ – $Rh_2O_3$ equilibrium, where $Rh_2O_3$ is the active site of the catalyst, is suggested.

The sulfur tolerance of the mono- and bimetallic (RhPt) catalysts was examined, and simulated fuels containing 4,6-DMDBT and $H_2S$ were evaluated as models for low-sulfur diesel (S < 10 ppm). The results obtained with 4,6-DMDBT correlated well with those for the commercial low-sulfur diesel, and the presence of heterocyclic sulfur compounds caused no more than slight deactivation of the bimetallic catalyst. The presence of $H_2S$, in contrast, caused immediate decrease in reforming and WGS activity of the RhPt catalyst, while the activity for oxidation reactions was not affected. Moreover, the adsorption of $H_2S$ blocked certain sites of the catalyst, hindering carbon deposition. The adsorption of $H_2S$ was mainly reversible and could be compensated with elevated temperature since the adsorption equilibrium of $H_2S$ was temperature dependent. In view of the different behaviour of the sulfur model compounds ($H_2S$ and 4,6-DMDBT) and the fact that $H_2S$ is not formed in ATR of low-sulfur diesel nor from 4,6-DMDBT, $H_2S$ can not be considered a suitable model compound for the heterocyclic sulfur compounds present in low-sulfur fuels.

In ATR of commercial low-sulfur diesel, $H_2$-rich fuel gas was successfully produced on the $2RhPt/ZrO_2$ catalyst at temperatures above 700 °C. Carbon deposition was stronger in ATR of low-sulfur diesel than of simulated fuel, however, owing to the complex nature of the fuel. The strong synergism between rhodium and platinum on the bimetallic catalysts, with the formation of a $Rh_xPt_{1-x}$ – $Rh_2O_3$ equilibrium, nevertheless

improved the catalyst performance (activity and selectivity for reforming, and tolerance for sulfur and coke deposition) over that of the monometallic catalysts.

In conclusion, a great potential exists for the development of active, selective and stable RhPt catalysts for hydrogen production units and large-scale fuel cell applications, where a wide range of liquid hydrocarbon fuels can be utilised as primary fuel. The operating conditions well depend on the characteristics of the primary fuel, where the types of hydrocarbons (i.e., aromatics) and sulfur compounds are critical.

## References


[1] Ferreira-Aparicio, P., Benito, M.J., Sanz, J.L., New trends in reforming technologies: from hydrogen industrial plants to multifuel microreformers, *Cat. Rev. – Sci. Eng.* **47** (2005) 491-588.

[2] Song, C., Fuel processing for low-temperature and high-temperature fuel cells – Challenges and opportunities for sustainable development in the 21st century, *Catal. Today* **77** (2002) 17-49.

[3] Strohm, J.J., Zheng, J., Song, C., Low-temperature steam reforming of jet fuel in the absence and presence of sulphur over Rh and Rh-Ni catalysts for fuel cells, *J. Catal.* **238** (2006) 309-320.

[4] Brown, L.F., A comparative study of fuels for on-board hydrogen production for fuel-cell-powered automobiles, *Int. J. Hydrogen Energy* **26** (2001) 381-397.

[5] Pettersson, L.J., Westerholm, R., State of the art of multi-fuel reformers for fuel cell vehicles: problem identification and research needs, *Int. J. Hydrogen Energy* **26** (2001) 243-264.

[6] Ogden, J.M., Steinbugler, M.M., Kreutz, T.G., A comparison of hydrogen, methanol and gasoline as fuels for fuel cell vehicles: implications for vehicle design and infrastructure development, *J. Power Sources* **79** (1999) 143-168.

[7] Krumpelt, M., Krause, T.R., Carter, J.D., Kopasz, J.P., Ahmed, S., Fuel processing for fuel cell systems in transportation and portable power applications, *Catal. Today* **77** (2002) 3-16.

[8] Ahmed, S., Krumpelt, M., Hydrogen from hydrocarbon fuels for fuel cells, *Int. J. Hydrogen Energy* **26** (2001) 291-301.

[9] Uemiya, S., Brief review of steam reforming using a metal membrane reactor, *Top. Catal.* **29** (2004) 79-84.

[10] Joensen, F., Rostrup-Nielsen, J.R., Conversion of hydrocarbons and alcohols for fuel cells, *J. Power Sources* **105** (2002) 195-201.

[11] Clarke, S.H., Dicks, A.L., Pointon, K., Smith, T.A., Swann, A., Catalytic aspects of the steam reforming of hydrocarbons in internal reforming fuel cells, *Catal. Today* **38** (1997) 411-423.

[12] Singhal, S.C., Kendall, K., Introduction to SOFCs. In: *High temperature solid oxide fuel cells: Fundamentals, design and application*s, eds. S.C. Singhal, K. Kendall, Elsevier, Cornwall 2003, pp. 1-22.

[13] Service, R.F., The hydrogen backlash, *Science* **305** (2004) 958-961.

[14] Roine, A., HSC Chemistry for Windows 5.11. Outokumpu Research Oy, 2003.

[15] Cheekatamarla, P., Lane, A.M., Catalytic autothermal reforming of diesel fuel for hydrogen generation in fuel cells I. Activity tests and sulfur poisoning, *J. Power Sources* **152** (2005) 256-263.

[16] Rostrup-Nielsen, J.R., New aspects of syngas production and use, *Catal. Today* **63** (2000) 159-164.

[17] Rostrup-Nielsen, J.R., Catalytic steam reforming. In: *Catalysis: Science and technology*, Vol. 5, eds. J.R. Anderson, M. Boudart, Springler Verlag, Berlin, Heidelberg, New York, Tokyo 1984, pp. 1-117.

[18] Rostrup-Nielsen, J.R., Bak Hansen, J.-H., Aparigio, L.M., Reforming of hydrocarbons into synthesis gas on supported metal catalysts, *Sekiyu Gakkaishi* **40** (1997) 366-377.

[19] Knudsen, J., Nilekar, A.U., Vang, R.T., Schnadt, J., Kunkes, E.L., Dumesic, J.A., Mavrikakis, M., Besenbacher, F., A Cu/Pt near-surface alloy for water-gas shift catalysis, *J. Am. Chem. Soc.* **129** (2007) 6485-6490.

[20] Panagiotopoulou, P., Kondarides, D., Effect of the nature of the support on the catalytic performance of noble metal catalysts for water-gas shift reaction, *Catal. Today* **112** (2006) 49-52.

[21] Aasberg-Petersen, K., Bak Hansen, J.-H., Christensen, T.S., Dybkjaer, I., Seier Christensen, P., Stub Nielsen, C., Winter Madsen, S.E.L., Rostrup-Nielsen, J.R., Technologies for large-scale gas conversion, *Appl. Catal., A* **221** (2001) 379-387.

[22] Naidja, A., Krishna, C.R., Butcher, T., Mahajan, D., Cool flame partial oxidation and its role in combustion and reforming of fuels for fuel cell systems, *Prog. Energy Combust. Sci.* **29** (2003) 155-191.

[23] Ormerod, R.M., Fuels and fuel processing. In: *High temperature solid oxide fuel cells: Fundamentals, design and applications*, eds. S.C. Singhal, K. Kendall, Elsevier, Cornwall 2003, pp. 333-361.

[24] Kochloefl, K., Steam reforming. In: *Handbook of heterogeneous catalysis*, Vol. 4, eds. G. Ertl, H. Knözinger, J. Weitkamp, VCH, Weinheim 1997, pp. 1819-1831.

[25] Rostrup-Nielsen, J.R., Conversion of hydrocarbons and alcohols for fuel cells, *Phys. Chem. Chem. Phys.* **3** (2001) 283-288.

[26] Bej, S.K., Maity, S.K., Turaga, U.T., Search for an efficient 4,6-DMDBT hydrodesulphurization catalyst: A review of recent studies, *Am. Chem. Soc.* **18(5)** (2004) 1227-1237.

[27] Suzuki, T., Iwanami, H.-I., Yoshinari, T., Steam reforming of kerosene on $Ru/Al_2O_3$ catalyst to yield hydrogen, *Int. J. Hydrogen Energy* **25** (2000) 119-126.

[28] Kirimura, K., Furuya, T., Sato, R., Ishii, Y., Kino, K., Usami, S., Bio-desulphuration of naphtothiophene and benzothiophene through selective cleavage of carbon-sulphur bonds by Rhodococcus sp. Strain WU-K2R, *Appl. Environ. Microbiol.* **68** (2002) 3867-3872.

[29] Rozanska, X., van Santen, R., Hutschka, F., Hafner, J., A periodic DFT study of the isomerisation of thiophenic derivatives catalyzed by acidic mordenite, *J. Catal.* **205** (2002) 388-397.

[30] Shekhawat, D., Berry, D.A., Gardner, T.H., Spivey, J.J., Catalytic reforming of liquid hydrocarbon fuels for fuel cell applications. In: *Catalysis*, Vol. 19, eds. J.J. Spivey, K.M. Dooley, Royal Society of Chemistry, London 2006, pp. 184-253.

[31] Trimm, D.L., Önsan, Z.I., Onboard fuel conversion for hydrogen-fuel-cell-driven vehicles, *Cat. Rev. - Sci. Eng.* **43** (2001) 31-84.

[32] Hennings, U., Reimert, R., Noble metal catalysts supported on gadolinium doped ceria used for natural gas reforming in the fuel cell applications, *Appl. Catal., B.* **70** (2007) 498-508.

[33] Cheekatamarla, P.K., Lane, A.M., Efficient sulphur-tolerant bimetallic catalysts for hydrogen generation from diesel fuel, *J. Power Sources* **153** (2006) 157-164.

[34] Trimm, D.L., Coke formation and minimisation during steam reforming reactions, *Catal. Today* **37** (1997) 233-238.

[35] Irusta, S., Cornaglia, L.M., Lombardo, E.A., Hydrogen production using Ni-Rh on $ZrO_2$ as potential low-temperature catalysts for membrane reactors, *J. Catal.* **210** (2002) 263-272.

[36] Claridge, J.B., Green, M.L.H., Tsang, S.C., York, A.P.E., Ashcroft, A.T., Battle, P.D., A study of carbon deposition on catalysts during the partial oxidation of methane to synthesis gas, *Catal. Lett.* **22** (1993) 299-305.

[37] Cheekatamarla, P.K., Finnerty, C.M., Reforming catalysts for hydrogen generation in fuel cell applications, *J. Power Sources* **160** (2006) 490-499.

[38] Anon, London Metal Exchange, Primary Nickel, Official Prices for 11 Apr 2008, *http://www.lme.co.uk/nickel.asp*, April 14, 2008.

[39] Anon, Kitco Inc., Historic Charts, *http://www.kitco.com/charts/*, April 11, 2008.

[40] Bagot, P.A.J., Cerezo, A., Smith, G.D.W., 3D atom probe study of gas adsorption and reaction on alloy catalyst surfaces II: Results on Pt and Pt-Rh, *Surf. Sci*. **601** (2007) 2245-2255.

[41] Oliver, C.P., King, B.V., O'Connor, D.J., Thin film growth of Pt on Rh(100): a LEIS study, *Surf. Sci.* **557** (2004) 101-108.

[42] Bernal, S., Botana, F.J., Calvino, J.J., Ciferdo, G.A., Pérez-Omil, J.A., Pintado, J.M., HREM study of the behaviour of a $Rh/CeO_2$ catalyst under high temperature reducing and oxidizing conditions, *Catal. Today* **23** (1995) 219-250.

[43] Ozturk, O., Park, J.B., Ma, S., Ratliff, J.S., Zhou, J., Mullins, D.R., Chen, D.A., Probing the interactions of Pt, Rh and bimetallic Pt-Rh clusters with the $TiO_2$(110) support, *Surf. Sci.* **601** (2007) 3099-3113.

[44] Cronauer, D.C., Krause, T.R., Salinas, J., Wagner, A., Wagner, J., Comparison of Rh, Pt, and Rh-Pt supported an oxide-ion conducting substrate as catalysts for autothermal reforming of methane, *Prepr. Pap.-Am. Chem. Soc., Div. Fuel Chem.* **51(1)** (2006) 297-299.

[45] Tanaka, K., Sasahara, A., Reconstructive activation of bimetallic surfaces: Catalytic reduction of NO with $H_2$ on Pt(100), Pt(110), Rh(100), Rh(110) and bimetallic single crystal surfaces of Rh/Pt(100), Rh/Pt(110), Pt/Rh(100), and Pt/Rh(110), *J. Mol. Catal. A: Chem.* **155** (2000) 13-22.

[46] Williams, F.L., Nelson, G.C., Surface composition of Pt/Rh alloys, *Appl. Surf. Sci.* **3** (1979) 409-415.

[47] Hu, Z., A Pt-Rh synergism in Pt/Rh three-way catalysts, *Chem. Commun.* **7** (1996) 879-880.

[48] Tzou, M.S., Asakura, K., Yamazaki, Y., Kuroda, H., Zeolite supported PtRh catalysts for CO oxidation and NO reduction: Evidence for bimetallic particles formation and synergism effect, *Catal. Lett.* **11** (1991) 33-40.

[49] Celio, H., Trenary, M., Robota, H.J., Comparative IR study of ethylene adsorption on a PtRh alloy and monometallic Pt and Rh catalysts supported on $Al_2O_3$. Identification of alloy-specific binding sites, *J. Phys. Chem.* **99** (1995) 6024-6028.

[50] Mizuno, T., Matsumura, Y., Nakajima, T., Mishima, S., Effect of support on catalytic properties of Rh catalysts for steam reforming of 2-propanol, *Int. J. Hydrogen Energy* **28** (2003) 1393-1399.

[51] Igarashi, A., Ohtaka, T., Motoki, S., Low-temperature steam reforming of n-butane over Rh and Ru catalysts supported on $ZrO_2$, *Catal. Lett.* **13** (1991) 189-194.

[52] Nagoaki, K., Seshan, K., Aika, K., Lercher, J.A., Carbon deposition during carbon dioxide reforming of methane – Comparison between $Pt/Al_2O_3$ and $Pt/ZrO_2$, *J. Catal.* **197** (2001) 34-42.

[53] Yamaguchi, T., Application of $ZrO_2$ as a catalyst and a catalyst support, *Catal. Today* **20** (1994) 199-218.

[54] Tanabe, K., Yamaguchi, T., Acid-base bifunctional catalysis by $ZrO_2$ and its mixed oxides, *Catal. Today* **20** (1994) 185-198.

[55] Burch, R., Loader, P.K., An investigation of the use of zirconia as a support for rhodium catalysts, *Appl. Catal., A* **143** (1996) 317-335.

[56] Yasuda, H., Masubayashi, N., Sato, T., Yoshimura, Y., Confirmation of sulfur

tolerance of bimetallic Pd-Pt supported on highly acidic USY zeolite by EXAFS, *Catal. Lett.* **54** (1998) 23-27.

[57] Tate, J.D., Jaakkola, P., The use of a portable low-resolution FT-IR for industrial gas analysis, *J. Process Anal. Chem.* **5** (2000) 15-28.

[58] Flytzani-Stephanopoulos, M., Voecks, G.E., Autothermal reforming of aliphatic and aromatic hydrocarbon liquids, *Int. J. Hydrogen Energy* **8(7)** (1983) 539-548.

[59] Highfield, J., Loo, Y.S., Zhong, Z., Grushko, B., Thermogravimetric studies of carbon nanofiber formation from methane at low temperature over Ni-based skeletal catalysts and the effect of substrate pre-carburization, *Carbon* **45** (2007) 2597-2607.

[60] Iojoiu, E.E., Domine, M.E., Davidia, T., Guilhaume, N., Mirodatos, C., Hydrogen production by sequential cracking of biomass-derived pyrolysis oil over noble metal catalysts supported on ceria-zirconia, *Appl. Catal., A* **323** (2007) 147-161.

[61] Bitter, J.H., Seshan, K., Lercher, J.A., Mono and bifunctional pathways of $CO_2/CH_4$ reforming over Pt and Rh based catalysts, *J. Catal.* **176** (1998) 93-101.

[62] Souza, M.M.V.M., Schmal, M., Methane conversion to synthesis gas by partial oxidation and $CO_2$ reforming over supported platinum catalysts, *Catal. Lett.* **91** (2003) 11-17.

[63] Fornasiero, P., Kaspas, J., Sergo, V., Graziani, M., Redox behavior of high-surface-area Rh-, Pt-, and Pd-loaded $Ce_{0.5}Zr_{0.5}O_2$ mixed oxide, *J. Catal.* **182** (1999) 56-69.

[64] Palm, C., Cremer, P., Peters, R., Stolten, D., Small-scale testing of precious metal catalyst in the autothermal reforming of various hydrocarbon feeds, *J. Power Sources* **106** (2002) 231-237.

[65] Rostrup-Nielsen, J.R., Sulfur-passivated nickel catalysts for carbon-free steam reforming of methane, *J. Catal.* **85** (1984) 31-43.

[66] Kolb, B., Müller, S., Botts, D.B., Hart, G.L.W., Ordering tendencies in the binary alloys of Rh, Pd, Ir, and Pt: Density functional calculations, *Phys. Rev. B* **74**, 144206 (2006) 1-7.

[67] Schlamp, G., Platinum group metals and compounds. In: *Ullmann's encyclopedia of industrial chemistry*, John Wiley & Sons, Inc. Last updated: 30 Aug. 2007, p. 42.

[68] Jacob, K.T., Priya, S., Waseda, Y., Thermodynamic properties and phase equilibria for Pt-Rh alloys, *Metall. Mater. Trans. A* **29A** (1998) 1545-1550.

[69] Jacob, K.T., Priya, S., Waseda, Y., Alloy-oxide equilibria in the system Pt-Rh-O, *Bull. Mater. Sci.* **21** (1998) 99-103.

[70] Hebenstreit, E.L.D., Hebenstreit, W., Schmid, M., Varga, P., $Pt_{25}Rh_{75}$(111), (110), and (100) studied by scanning tunnelling microscopy with chemical contrast, *Surf. Sci.* **441** (1999) 441-453.

[71] Tanaka, K., Chemical reconstruction and catalysis of metal and bimetallic surfaces, *Surf. Sci.* **357-358** (1996) 721-728.

[72] Greeley, J., Mavrikakis, M., Alloy catalysts designed from first principles, *Nat. Mater.* **3** (2004) 810-815.

[73] Ferrandon, M., Krause, T., Role of the oxide support on the performance of Rh catalysts for the autothermal reforming of gasoline and gasoline surrogates to hydrogen, *Appl. Catal., A* **311** (2006) 135-145.

[74] Bernal, S., Calvino, J.J., Cauqui, M.A., Gatica, J.M., Larese, C., Perez Omil, J.A., Pintado, J.M., Some recent results on metal/support interaction effects in NM/$CeO_2$ (NM: noble metal) catalysts, *Catal. Today* **50** (1999) 175-206.

[75] Ashcroft, N.W., Mermin, N.D., Crystal lattices. In: *Solid state physics*, ed. D.G. Crane, Holt, Rinehart and Winston, Philadelphia 1976, pp. 63-83.

[76] Zhu, L., Wang, R., King, T.S., DePristo, A.E., Effects of chemisorption on the surface composition of bimetallic catalysts, *J. Catal.* **167** (1997) 408-411.

[77] Beck, D.D., Capehart, T.W., Wong, C., Belton, D.N., XAFS characterization of rhodium/alumina after treatment in high-temperature oxidizing environments, *J. Catal.* **144(1)** (1993) 311-324.

[78] Suopanki, A., Polvinen, R., Valden, M., Härkönen, M., Rh oxide reducibility and catalytic activity of model Pt–Rh catalysts, *Catal. Today* **100** (2005) 327-330.

[79] Hoang, D.L., Leiske, H., Effect of hydrogen treatments on $ZrO_2$ and $Pt/ZrO_2$ catalysts, *Catal. Lett.* **27** (1994) 33-42.

[80] Zhou, S., Varughese, B., Eichhorn, B., Jackson, G., McIlwrath, K., Pt-Cu core-shell and alloy nanoparticles for heterogeneous $NO_x$ reduction: Anomalous stability and reactivity of a core-shell nanostructure, *Angew. Chem. Int. Ed.* **44** (2005) 4539-4543.

[81] Cimini, F., Prins, R., Influence of the Pt/Rh molar ratio on the final structure of bimetallic RhPt clusters supported on NaY zeolite, *J. Phys. IV* **7** (1997) 925-926.

ISBN 978-951-22-9570-8
ISBN 978-951-22-9571-5 (PDF)
ISSN 1795-2239
ISSN 1795-4584 (PDF)